Noname manuscript No.
(will be inserted by the editor)

Random walk methods for modeling hydrodynamic transport in porous and fractured media from pore to reservoir scale

Benoit Noetinger · Delphine Roubinet · Anna Russian · Tanguy Le Borgne · Frederick Delay · Marco Dentz · Jean-Raynald de Dreuzy · Philippe Gouze

Abstract Random walk (RW) methods are recurring Monte Carlo methods used to model convective and diffusive transport in complex heterogeneous media. Many applications can be found, including fluid mechanic, hydrology, and chemical reactors modeling. These methods are easy to implement, very versatile and flexible enough to become appealing for many applications because they generally overlook or deeply simplify the building of explicit complex meshes required by deterministic methods. RW provide a good physical understanding of the interactions between the space scales of heterogeneities and the transport phenomena under consideration. In addition, they can result in efficient up-scaling methods, especially in the context of flow and transport in fractured media. In the present study, we review the applications of RW to several situations that cope with diverse spatial scales, and different insights into up-scaling problems. The advantages and down-

B. Noetinger
IFPEN 1-4 avenue de Bois Préau, 92852, France
E-mail: benoit.noetinger@ifpen.fr

D. Roubinet
Applied and Environmental Geophysics Group, Institute of Earth Sciences, University of Lausanne, 1015 Lausanne, Switzerland

A. Russian
Géosciences, Université de Montpellier 2, CNRS

T. le Borgne
Université de Rennes 1, CNRS, Géosciences Rennes, UMR 6118, Rennes, France

F. Delay
Laboratoire dHydrologie et de Géochimie de Strasbourg, Univ. Strasbourg/EOST, CNRS UMR 7517, 1 rue Blessig, 67000 Strasbourg, France

M. Dentz
Institute of Environmental Assessment and Water Research, Spanish National Research Council, Barcelona, Spain

J.R. de Dreuzy
Géosciences Rennes, CNRS, UMR 6118, Rennes, France

P. Gouze
Géosciences, Université de Montpellier 2, CNRS

sides of RW are also discussed, thus providing a few avenues for further works and applications.

Keywords Random walk · Random Media · Fractured media · Diffusion · Dispersion · Up-scaling · Transfers · Multiple Porosity

1 Introduction

In the early 20 th century, thanks to seminal contributions of major scientists such as Einstein, Langevin, le Chatelier and Wiener among others, the Random walk (RW) approach introduced the first quantified depiction of brownian motion which resulted in a fruitful microscopic picture of the diffusion mechanism (Scher et al, 2002a). The conceptual simplicity of RW associated with its easiness of implementation were conductive to a fast dissemination of associated techniques and algorithms in many areas of science, from biology and colloidal science to modern finance, including statistical physics, chemical engineering, and geosciences. Regarding the latter topic, many applications can be found in the field of hydrology, oil and gas industry or subsurface repository of various wastes. As an illustration, RW techniques can also be employed as a direct simulation technique for passive tracer or pollutant transport in aquifers (Kinzelbach, 1988; Kinzelbach and Uffink, 1991; Zimmermann et al, 2001; Hoteit et al, 2002b; Delay et al, 2005). At the laboratory scale, the recent advances in the imaging techniques of rock textures provide high resolution pictures of the pore space (Nunes et al, 2015). This very exhaustive and complex information needs for post-processing aimed at inferring effective transport properties in porous media such as permeability, porosity, and electrical conductivity, to mention a few. For example, electrical conductivity was first computed using RW by Kim and Torquato (1992) and several authors ((Sahimi, 2011) and reference therein). At the same pore-to-sample scale, RW techniques were also used to interpret Nuclear Magnetic Resonance (NMR) data (Néel et al, 2011, 2014; Guillon et al, 2013, 2014; Fleury et al, 2015). At a larger scale, typically from m to km, a major issue of various applications, especially those performing flow and transport simulations in subsurface reservoirs, is the capability of accounting for the detailed natural variability of the host medium with the maximum accuracy over objects of large sizes (typically several km in the case of aquifers or oil & gas reservoirs). These applications range from a better understanding of the fate of pollutants in the subsurface, to improving oil and gas recovery. At the large scale, most calculations are still performed using Finite Volume, Finite Difference or Finite Element approaches requiring a high resolution and cumbersome meshing to represent the geometry of the modeled domain. However, because the size of an elementary mesh is often too large, discrete descriptions of the domain may also require the availability of effective transport equations at the scale of the mesh and accounting for eventual unresolved sub-grid scale effects. In most cases, it is assumed that transport is still ruled by the Advection Dispersion Equation (ADE) which is of questionable validity at the small scale (Matheron and de Marsily, 1980; Bouchaud and Georges, 1990; Berkowitz and Scher, 1998; Berkowitz et al, 2000; Scher et al, 2002a; Néel et al, 2011). In addition, the parameters associated with flow and transport are usually poorly known a priori and have to be inferred by facing model outputs with available data. RW techniques are good

candidates for both identifying sub-grid effects and parameters (Berkowitz and Balberg, 1993; Néel et al, 2011). In particular, obtaining valuable descriptions of transport in low permeability media concealing widespread heterogeneities involving stagnant zones, adsorption and chemical reactions properties is of major interest. These highly disordered media can exhibit very rich anomalous transport properties preventing any classical description relying upon standard Darcy's law and ADE. RW methods can for instance represent "fractional derivative" transport equation accounting for memory effects over wide ranges of time (Matheron and de Marsily, 1980; O'Shaughnessy and Procaccia, 1985; Charlaix et al, 1987; Barker, 1988; Chang and Yortsos, 1990; Bouchaud and Georges, 1990; Metzler et al, 1994; Noetinger and Gautier, 1998; Metzler and Klafter, 2000). In the extreme case of fractured media, Continuous Time Random Walk (CTRW) or Time Domain Random Walk (TDRW) algorithms techniques were successfully employed to determine transfer functions that are key for implementing the so called dual porosity models (Noetinger and Estebenet, 2000; Noetinger et al, 2001a,b).

RW algorithms are very well suited to capture the motion and the spreading of a diffusive set of particles representing a tracer plume in an advecting flow field. The rather subtle interplay between molecular diffusion and the heterogeneous velocity field can be simulated directly, resulting in a clear physical interpretation of the relevant characteristic times and scales prevailing during transport. Analytical results of the Taylor and Aris (Taylor, 1954; Aris, 1956) dispersion can be retrieved (Salles et al, 1993). In turn, these results can be used to estimate dispersivity in more complex geometries. In the case of spatially varying diffusion coefficients, including discontinuous cases, the RW may experience some difficulties. To avoid spurious accumulation of particles in low diffusivity zones, some "reflection rules" have to be imposed at the locations of discontinuities (Kinzelbach, 1988; Kinzelbach and Uffink, 1991; Hoteit et al, 2002b). In addition, the algorithm can become inefficient in low diffusivity zones because the spatial time step needed for an accurate resolution of transport can become very small. Both issues can be corrected using suitable time step increments that avoid expansive and unnecessary iterations in low velocity and low diffusion zones. The main idea is using fixed spatial meshes instead of even time steps. In that framework, RW methods loose their original "meshless character", and are found to be connected to usual Finite Volume schemes. This leads to model diffusion over a fixed lattice or graph that can be built with standard meshing tools. For its part, the residence time at a given site becomes a random variable, with the consequence that the resulting algorithm belongs to a wider class of techniques, namely the Time Domain Random Walk (TDRW). These TDRW algorithms are also particularly well suited to implementations on highly parallel computing resources. An additional interest is that the resulting formulation is quite close to the classical solutions as that provided by standard numerical analysis. Anomalous dispersion effects mainly due to the persistence of large scale correlations in a flow field can thus be simulated using RW with suitable kernels (Berkowitz and Scher, 1998; Berkowitz et al, 2000; Néel et al, 2011; Scher et al, 2002a,b). For their numerical part, RW methods can be implemented using structured or unstructured meshes, which allows to tackle the problem of diffusion in very complex media, including fracture networks (Noetinger and Estebenet, 2000; Noetinger et al, 2001a,b; Roubinet et al, 2010, 2013). Adsorption phenomena, as well as chemical reactions can also be accounted for. By nature, RW methods are very well suited for highly

parallel computing architectures which reveals useful to perform calculations over complex domains or when moving multiple reacting species in solution.

RW methods provide interesting insights into transport mechanisms that can enlighten us about our understanding of mixing processes in disordered flows. In the case of fractured media, a careful interpretation of the output of RW simulations give efficient and direct tools to parameterize multiple porosity large scale models by way of a complete determination of transient transfer functions (Noetinger and Estebenet, 2000; Noetinger et al, 2001a,b; Roubinet et al, 2010, 2013). These functions can thus help to pattern multiple rate transfer models (Haggerty and Gorelick, 1995) or Multiple Interacting Continua (MINC) models (Narasimhan and Pruess, 1988). Characteristic exponents associated with anomalous diffusion/dispersion processes can be estimated using RW methods (de Arcangelis et al, 1986; Berkowitz and Scher, 1997; McCarthy, 1993a; Koplik et al, 1988; Bouchaud and Georges, 1990), as well as the REV or mixing lengths, even if large scale practical simulations still remain the playing field of conventional meshed models.

The goal of the present paper is to review the state of the art regarding applications of RW, TDRW or CTRW to the up scaling of flows and mass transfers in heterogeneous and fractured media.

The contribution is organized as follows. We first review in section 2.4 the underlying theory of RW algorithms for solving an advection diffusion equation. We focus on TDRW that solves spatially discretized equations having the same form than those arising from Finite Volume discretization of advection dispersion operators. Next, numerical issues are addressed, from fully coupled advection dispersion diffusion equations 3 to purely diffusive issues including heterogeneous, fractured media and the double porosity large scale description 3.3. These models can be generalized to Multiple Rate Transfer Models involving transfer functions between the matrix and the fractures that can be evaluated using TDRW techniques. In a next section 3.5, application of RW to understanding and modeling mixing are discussed. Applications from pore to field scale 4, including radial flows in the vicinity of wells are discussed. Finally, some other applications are discussed and some conclusions and avenues for future research are discussed.

2 Theoretical Background for Random Walk Methods

This section summarizes the basis on which random walk methods are built to describe solute transport in heterogeneous media. We start with classical or discrete time random walks, then briefly review its generalization to the continuous time random walk (CTRW) framework. Based on the CTRW approach, we report on the fundaments of the time domain random walk method (TDRW). Finally, we review the use of the CTRW as an averaging framework for transport in heterogeneous media.

2.1 Classical (Discrete-Time) Random Walks

Classical random walk particle tracking is based on the equivalence between the Fokker-Planck equation and the equation of motion of solute particles subject to

advective and diffusive-dispersive mass transfer. A general Fokker-Planck equation for the scalar quantity $P(\mathbf{x},t)$ can be written as (Risken, 1996)

$$\frac{\partial P(\mathbf{x},t)}{\partial t} + \nabla \cdot [\mathbf{v}(\mathbf{x})P(\mathbf{x},t)] + \nabla \otimes \nabla : [\mathbf{B}(\mathbf{x})P(\mathbf{x},t)] = 0, \tag{1}$$

where $\otimes$ denotes the outer and : the inner tensor product. The drift vector and dispersion tensor are denoted by $\mathbf{v}(\mathbf{x})$ and $\mathbf{B}(\mathbf{x})$, respectively. As shown in Appendix A, this Fokker-Planck equation is exactly equivalent to the Langevin equation

$$\frac{d\mathbf{x}(t)}{dt} = \mathbf{v}[\mathbf{x}(t)] + \sqrt{2\mathbf{B}[\mathbf{x}(t)]} \cdot \boldsymbol{\zeta}(t), \tag{2}$$

where $\sqrt{\mathbf{B}(\mathbf{x})}$ is the square-root of the tensor $\mathbf{B}(\mathbf{x})$, $\boldsymbol{\zeta}(t)$ denotes a Gaussian white noise characterized by zero mean $\langle \boldsymbol{\zeta}(t) \rangle = \mathbf{0}$ and variance $\langle \zeta_i(t)\zeta_j(t') \rangle = \delta_{ij}\delta(t-t')$. The angular brackets denote the noise average over all particles. The particle distribution $P(\mathbf{x},t)$ can be written in terms of the particle trajectories $\mathbf{x}(t)$ as

$$P(\mathbf{x},t) = \langle \delta[\mathbf{x} - \mathbf{x}(t)] \rangle. \tag{3}$$

We name this modeling approach as a discrete time random walk because particle positions are incremented in constant time intervals as

$$\mathbf{x}(t+dt) = \mathbf{x}(t) + \mathbf{v}[\mathbf{x}(t)]dt + \sqrt{2\mathbf{B}[\mathbf{x}(t)]} \cdot \boldsymbol{\eta}(t), \qquad \boldsymbol{\eta}(t) = \int_t^{t+dt} dt' \boldsymbol{\zeta}(t'). \tag{4}$$

Note that we use here the Ito interpretation of the stochastic integral (Risken, 1996). The random increment $\boldsymbol{\eta}(t)$ has zero mean and variance $\langle \eta_i(t)\eta_j(t) \rangle = \delta_{ij}dt$.

Solute or heat transport as well as hydraulic head propagation in a heterogeneous porous medium are not in general described by a Fokker-Planck equation of the form (1), but the advection dispersion equation (ADE) for the scalar $c(\mathbf{x},t)$

$$\phi(\mathbf{x})\frac{\partial c(\mathbf{x},t)}{\partial t} + \nabla \cdot [\mathbf{u}(\mathbf{x})c(\mathbf{x},t)] - \nabla \cdot [\mathbf{D}(\mathbf{x})\nabla c(\mathbf{x},t)] = 0. \tag{5}$$

For solute transport $c(\mathbf{x},t)$ denotes the concentration, $\phi(\mathbf{x})$ is the porosity and $\mathbf{D}(\mathbf{x})$ is the hydrodynamic dispersion tensor. For hydraulic head propagation, we set the flow velocity $\mathbf{u}(\mathbf{x}) = \mathbf{0}$, $\phi(\mathbf{x})$ denotes the specific storage and $\mathbf{D}(\mathbf{x})$ is the hydraulic conductivity tensor. It is important to note that $c(\mathbf{x},t)$ in (5) is not a conserved quantity because it is $\phi(\mathbf{x})c(\mathbf{x},t)$ that is conserved. Thus, introducing

$$P(\mathbf{x},t) = \phi(\mathbf{x})c(\mathbf{x},t), \tag{6}$$

which satisfies the equation

$$\frac{\partial P(\mathbf{x},t)}{\partial t} + \nabla \cdot \left[\frac{\mathbf{u}(\mathbf{x})}{\phi(\mathbf{x})}P(\mathbf{x},t)\right] - \nabla \cdot \left[\mathbf{D}(\mathbf{x})\nabla\frac{P(\mathbf{x},t)}{\phi(\mathbf{x})}\right] = 0. \tag{7}$$

We can reformulate this equation in the form of the Fokker-Planck equation (1) as

$$\frac{\partial P(\mathbf{x},t)}{\partial t} + \nabla \cdot \left[\frac{\mathbf{u}(\mathbf{x})}{\phi(\mathbf{x})} + \frac{\nabla \cdot \mathbf{D}(\mathbf{x})}{\phi(\mathbf{x})}\right] P(\mathbf{x},t) - \nabla \otimes \nabla : \left[\frac{\mathbf{D}(\mathbf{x})}{\phi(\mathbf{x})}P(\mathbf{x},t)\right] = 0. \tag{8}$$

Through the equivalence between (1) and (2), we find the Langevin equation that is equivalent to (5) as (Kinzelbach, 1988)

$$\frac{d\mathbf{x}(t)}{dt} = \frac{\mathbf{u}[\mathbf{x}(t)]}{\phi[\mathbf{x}(t)]} + \frac{\nabla \cdot \mathbf{D}[\mathbf{x}(t)]}{\phi[\mathbf{x}(t)]} + \sqrt{\frac{2\mathbf{D}[\mathbf{x}(t)]}{\phi[\mathbf{x}(t)]}} \cdot \boldsymbol{\zeta}(t). \tag{9}$$

The solute concentration $c(\mathbf{x}, t)$ is given in terms of the particle trajectories through (3) and (6) as

$$c(\mathbf{x}, t) = \frac{\langle \delta[\mathbf{x} - \mathbf{x}(t)] \rangle}{\phi(\mathbf{x})}. \tag{10}$$

2.2 Continuous Time Random Walks

We present here a generalization of the previous depiction of discrete time random walk to continuous time (Berkowitz et al, 2002, 2006). The particle position and time are now incremented at each random walk step as

$$\mathbf{x}_{n+1} = \mathbf{x}_n + \mathbf{A}(\mathbf{x}_n), \qquad t_{n+1} = t_n + \tau(\mathbf{x}_n). \tag{11}$$

The random space and time increments $\mathbf{A}(\mathbf{x}_n)$ and $\tau(\mathbf{x}_n)$ depend in general on the particle position and they can be coupled (Scher and Lax, 1973a), and characterized by their joint probability density function (PDF) $\psi(a, t; \mathbf{x})$. Notice that both space and time are continuous variables. The particle density $P(\mathbf{x}, t)$ can be described by the following system of equations (Berkowitz et al, 2002; Srinivasan et al, 2010)

$$P(\mathbf{x}, t) = \int_0^t dt' R(\mathbf{x}, t') \int_{t-t'}^{\infty} dt'' \psi(t''; \mathbf{x}) \tag{12a}$$

$$R(\mathbf{x}, t) = P(\mathbf{x}, t)\delta(t) + \int d\mathbf{a} \int_0^t dt' \psi(\mathbf{a}, t'; \mathbf{x} - \mathbf{a}) R(\mathbf{x} - \mathbf{a}, t - t'). \tag{12b}$$

The first equation states that the probability of a particle to be in the volume $[\mathbf{x}, \mathbf{x} + d\mathbf{x}]$ at time t is equal to the probability $R(\mathbf{x}, t')$ that the particle just arrive in the volume $[\mathbf{x}, \mathbf{x} + d\mathbf{x}]$ at a time in $[t', t' + dt']$ and remains there for the duration of $t - t'$. The marginal PDF of transition times is given by

$$\psi(t; \mathbf{x}) = \int d\mathbf{a} \psi(\mathbf{a}, t; \mathbf{x}). \tag{13}$$

The second equation of 12 can be viewed as a Chapman Kolmogorov equation for the probability density $R(\mathbf{x}, t)$. The linear system (12) can be solved for the Laplace transform (Abramowitz and Stegun, 1972) of the particle density $P(\mathbf{x}, t)$, which gives after some algebra the integral equation:[1]

$$sP(\mathbf{x}, s) = P(\mathbf{x}, 0) + \int d\mathbf{a} \frac{s\psi(\mathbf{a}, s; \mathbf{x} - \mathbf{a})}{1 - \psi(s; \mathbf{x} - \mathbf{a})} P(\mathbf{x} - \mathbf{a}, s) \int d\mathbf{a} \frac{s\psi(\mathbf{a}, s; \mathbf{x})}{1 - \psi(s; \mathbf{x})} P(\mathbf{x}, s). \tag{14}$$

[1] To simplify notations, functions with "s" variables correspond to Laplace transforms throughout the rest of the paper.

Inverse Laplace transform gives the generalized Master equation (Kenkre et al, 1973)

$$\frac{dP(\mathbf{x},t)}{dt} = \int_0^t dt' \int d\mathbf{a} M(\mathbf{a},t;\mathbf{x}-\mathbf{a}) P(\mathbf{x}-\mathbf{a},t) - \int_0^t dt' \int d\mathbf{a} M(\mathbf{a},t;\mathbf{x}-\mathbf{a}) P(\mathbf{x},t), \tag{15}$$

where we define the memory function

$$M(\mathbf{a},s;\mathbf{x}) = \frac{s\psi(\mathbf{a},s;\mathbf{x})}{1-\psi(s;\mathbf{x})}. \tag{16}$$

Under the assumption that $M(\mathbf{a},t;\mathbf{x}-\mathbf{a})$ is sharply peaked around $\mathbf{0}$ the spatial convolution in (15) may be localized through a Taylor expansion of the integrand about $\mathbf{x}$ (Berkowitz et al, 2002) such that

$$\frac{\partial P(\mathbf{x},t)}{\partial t} + \int_0^t dt' \nabla \cdot \left[\boldsymbol{\nu}(\mathbf{x},t-t') P(\mathbf{x},t')\right] - \int_0^t dt' \nabla \otimes \nabla \cdot \left[\boldsymbol{\beta}(\mathbf{x},t-t') P(\mathbf{x},t')\right] + \cdots = 0, \tag{17}$$

where the dots represent higher order contributions in the moments of $M(\mathbf{a},t;\mathbf{x})$. Notably, the velocity and dispersion kernels $\boldsymbol{\nu}(\mathbf{x},t)$ and $\boldsymbol{\beta}(\mathbf{x},t)$ have been defined in (17) as

$$\boldsymbol{\nu}(\mathbf{x},t) = \int d\mathbf{a}\, \mathbf{a} M(\mathbf{a},t;\mathbf{x}), \qquad \boldsymbol{\beta}(\mathbf{x},t) = \int d\mathbf{a}\, \mathbf{a} \otimes \mathbf{a} M(\mathbf{a},t;\mathbf{x}). \tag{18}$$

2.3 Time Domain Random Walks

Time domain random walk (TDRW) methods have been used as efficient alternatives to discrete time random walks for the solution of solute transport and flow problems in heterogeneous media as described by (5). Complementary to the classical discrete time random walk approach, the TDRW fixes the spatial particle transition length and asks for the time that is needed to travel over this distance. This approach is obviously in the spirit of and inherits from the CTRW discussed in the previous section. Let us elucidate this relation by considering the ADE (5) discretized in space. Using a finite difference or a finite volume discretization, it can be written (Delay et al, 2002; Dentz et al, 2012; Russian et al, 2016)

$$\phi_i \frac{dc_i(t)}{dt} = \sum_{[ij]} b_{ij} c_j(t) - \sum_{[ij]} b_{ji} c_i(t), \tag{19}$$

where $c_i(t)$ is the concentration at voxel i. The notation $\sum_{[ij]}$ means summation over the nearest neighbors of voxel i. The coefficients b_{ij} are given in terms of

the flow velocity and dispersion coefficients as (Gjetvaj et al, 2015; Russian et al, 2016)

$$b_{ij} = \frac{\hat{D}_{ij}}{\xi^2} + \frac{|u_{ij}|}{2\xi}\left(\frac{u_{ij}}{|u_{ij}|} + 1\right), \tag{20}$$

with the discretization length ξ. For the sake of simplicity we assume that the discretization is uniform and that all grid cells, or voxels, have the same volume V and surface area S. The velocity component u_{ij} of $\mathbf{u}_j$ is the flow velocity at voxel j in direction of voxel i, that is $u_{ij} = \mathbf{u}_j \cdot \mathbf{e}_{ij}$, where the vector $\mathbf{e}_{ij}$ is oriented from j to i. Thus, $u_{ij} > 0$ implies that voxel i is downstream from voxel j, and vice versa. The dispersion coefficient $\hat{D}_{ij}$ measures the dispersive mass flux between voxels i and j. It is typically given by a suitable average of the dispersion coefficient in neighboring voxels (Noetinger and Estebenet, 2000; Dentz et al, 2012).

The equivalence with the CTRW approach can be evidenced by following Dentz et al (2012) and rewriting the generalized Master equation (15) in the discrete space,

$$\frac{dP_i(t)}{dt} = \int_0^t dt' \sum_{[ij]} \left[M_{ij}(t-t')P_j(t') - M_{ji}(t-t')P_i(t')\right], \tag{21}$$

where we assume that interactions of the modeled process only occur between nearest neighbors. Furthermore, we set $P(\mathbf{x}_i, t) = P_i(t)$ and $M(\mathbf{x}_i - \mathbf{x}_j, t; \mathbf{x}_j) = M_{ij}(t)$. We assume now that the transition pdf for length and time can be decoupled into $\psi_{ij}(t) = w_{ij}\psi_j(t)$ with w_{ij} the probability to make a transition from j to i. We also specify the transition time pdf as an exponential function (Scher and Lax, 1973a)

$$\psi_j(t) = \exp(-t/\tau_j)/\tau_j. \tag{22}$$

Thus, Laplace transform of the memory function $M_{ij}(t)$ simplifies to

$$M_{ij}(s) = \frac{w_{ij}}{\tau_j}. \tag{23}$$

The generalized Master equation then reads as

$$\frac{dP_i(t)}{dt} = \sum_{[ij]} \frac{w_{ij}}{\tau_j} P_j(t) - \sum_{[ij]} \frac{w_{ji}}{\tau_i} P_i(t). \tag{24}$$

By identifying $P_i(t) = \phi_i c_i(t)$ and $b_{ij} = w_{ij}\phi_j/\tau_j$, (19) and (24) become similar. In this sense, the discretized ADE (19) can be solved through a TDRW, whose transition probability in space and transition time are given by

$$w_{ij} = \frac{b_{ij}\tau_j}{\phi_j}, \qquad \tau_i = \frac{\phi_i}{\sum_{[ij]} b_{ji}}. \tag{25}$$

2.4 The Continuous Time Random Walk as an Average Transport Approach

The CTRW approach has been used as an upscaling framework to describe average transport in heterogeneous media (Klafter and Silbey, 1980; Berkowitz et al, 2006). The pioneering works of Scher and Lax (1973a) and Scher and Lax (1973b) model the transport of charge carries in impure semiconductors with a CTRW whose PDF of waiting times reflects some charge trapping in the potential wells created by charged impurities. This approach allowed for the explanation and prediction of observed charge currents, or in other words, arrival time distributions, that show the heavy tails characterizing anomalous transport. Since then, the CTRW has been used as an approach to model the history-dependent average dynamics in diverse types of fluctuating and disordered systems. One can mention: particle transport in media with both heterogeneity at the pore and Darcy scales (Berkowitz and Scher, 1998, 1997; Hatano and Hatano, 1998; Berkowitz et al, 2000; Cortis and Berkowitz, 2004; Le Borgne et al, 2008a; de Anna et al, 2013; Kang et al, 2014; Holzner et al, 2015), light dispersion in heterogeneous optical media (Barthelemy et al, 2008), the description of financial distributions, the motion and migrations of animals, and many more (Klafter and Sokolov, 2005).

In the context of average transport or transport upscaling for heterogeneous media, the CTRW maps the spatial distributions of the fluctuating medium properties onto the (joint) distribution of transition lengths and durations $\psi(\mathbf{a}, t)$. It is worth noticing that in general the joint PDF depends on the spatial position, as in sections 2.2 and 2.3. This spatial dependence is here homogenized by the ensemble average as outlined in Scher and Lax (1973a) and Scher and Lax (1973b). To illustrate this approach, we adopt the method reported in Appendix B of the paper by Scher and Lax (1973a) dealing with pure diffusion in a medium characterized by spatially distributed particle traps (see also, Bouchaud and Georges, 1990; Dentz et al, 2016). Our starting point is equation (19) for a medium that is characterized by constant and isotropic dispersion properties, but a spatially variable porosity or retardation coefficient ϕ_i, which quantifies the strength of the particle trap. Under these conditions, the coefficients b_{ij} in (20) simplify into

$$b = \frac{D}{\xi^2}. \tag{26}$$

Therefore, the CTRW for this transport system is characterized by the joint transition pdf

$$\psi_{ij}(t) = \frac{1}{2d}\psi_j(t), \qquad \psi_j(t) = \exp(-t/\tau_j)/\tau_j, \qquad \tau_j = \phi_j \tau_D, \tag{27}$$

where $\tau_D = \xi^2/D$, and d is the dimension of space. The CTRW equations (12) now rewrite as

$$P_i(t) = \int_0^t dt' R_i(t') \int_{t-t'}^{\infty} dt'' \psi_i(t'') \tag{28a}$$

$$R_i(t) = P_0(t)\delta(t) + \sum_{[ij]} \int_0^t dt' \frac{1}{2d}\psi_j(t-t')R_j(t'). \tag{28b}$$

The average transport behavior can be obtained by way of an ensemble averaging over the disorder, with the meaning here of averaging the distribution of ϕ_i. To this end, we assume that the ϕ_i at different sites i and j are uncorrelated. We remind that $R_i(t)$ represents the probability density that a particle just arrive at site i at time t. This probability conceals information on all the other sites visited before. We also remind that the average number of new sites visited for an isotropic lattice random walk in $d > 3$ spatial dimensions increases with the number of random walk steps (Bouchaud and Georges, 1990). This means that $R_i(t)$ and $\psi_i(t)$ can be assumed to be statistically independent because it is unlikely that a particle returns to the same site. Consequently, for $d = 3$ dimensions we can perform the ensemble average through the integration of (28) over the distribution $p_\phi(\phi)$ of point values of ϕ_i, which renders

$$\overline{P}_i(t) = \int_0^t dt' \overline{R}_i(t') \int_{t-t'}^{\infty} dt'' \psi(t'') \tag{29a}$$

$$\overline{R}_i(t) = P_0(t)\delta(t) + \sum_{[ij]} \int_0^t dt' \frac{1}{2d} \psi(t-t') \overline{R}_j(t'), \tag{29b}$$

where the pdf of transition times integrates the disorder distributions as

$$\psi(t) = \int_0^{\infty} d\phi p_\phi(\phi) \frac{\exp\left(-\frac{t}{\phi\tau_D}\right)}{\phi\tau_D}. \tag{30}$$

It is noteworthy that such an average transport description holds under the condition that the disorders experienced by the particle at subsequent steps are independent.

In this spirit, CTRW has been applied to advective and dispersive transport in heterogeneous media. For advection-dominated transport, the transition time τ is related to the advection travel time over a characteristic length ℓ, of the same order of magnitude as the correlation distance of the particle velocity along a streamline, i.e.,

$$\tau = \frac{\ell}{v}, \tag{31}$$

where v is the particle velocity. The spatial correlation properties of Lagrangian particle velocities along streamlines, and the representation of transport by CTRW have been studied for pore and Darcy scale transport (Le Borgne et al, 2008b,a; Kang et al, 2011; de Anna et al, 2013; Kang et al, 2014). The relation between the spatial distribution of hydraulic conductivity and transition times has been studied in Edery et al (2014). The CTRW as an average transport approach has been employed in the interpretation and prediction of diverse anomalous and non-Fickian behaviors observed in geological media (Berkowitz et al, 2006). In the following, we briefly summarize the behaviors of breakthrough curves and spatial concentration moments that are obtained within the CTRW framework for a transition time pdf that decays algebraically as $\psi(t) \propto t^{-1-\beta}$ with $0 < \beta < 2$.

2.4.1 Breakthrough Curves

Hydrodynamic transport in natural formations is frequently characterized by breakthrough curves that here depict the first passage time pdfs, or solute fluxes. Both forms of breakthroughs are quite similar in the case of advection-dominated transport. The first passage time $t(x_1)$ at a control plane located at x_1 can be formulated in terms of particle trajectories as

$$t(x_1) = \inf[t|x(t) \geq x_1]. \tag{32}$$

The pdf of first passage times can then be written as

$$f(t, x_1) = \langle \delta[t - t(x_1)] \rangle. \tag{33}$$

For an instantaneous particle injection into an infinite or semi-infinite domain, it has been found (Berkowitz et al, 2006) that $f(t, x_1)$ scales as the transition time pdf,

$$f(t, x_1) \propto t^{-1-\beta}. \tag{34}$$

2.4.2 Spatial Concentration Moments

Other observables characterizing the global plume behavior can be found in the first and second centered moments of the solute spatial distribution. The first $m_i^{(1)}$ and second $m_{ij}^{(2)}$ spatial moments of $P(\mathbf{x}, t)$ are defined as

$$m_i^{(1)}(t) \equiv \int d^d x \, x_i P(\mathbf{x}, t) \qquad m_{ij}^{(2)}(t) \equiv \int d^d x \, x_i x_j P(\mathbf{x}, t). \tag{35}$$

In terms of the particle trajectories, these moments are given by $m_i^{(1)}(t) = \langle x_i(t) \rangle$ and $m_{ij}^{(2)}(t) = \langle x_i(t) \, x_j(t) \rangle$. The second centered moments are a measure of the global plume width, and are defined by

$$\kappa_{ij}(t) = m_{ij}^{(2)}(t) - m_i^{(1)}(t) m_j^{(1)}(t). \tag{36}$$

With concern to the behavior in time of the spatial moments, we distinguish the range of β values between 0 and 1 from the range between 1 and 2. For $0 < \beta < 1$ it has been found that (Berkowitz et al, 2006)

$$m_1(t) \propto t^{\beta}, \qquad \kappa_{11}(t) \propto t^{2\beta}, \qquad \kappa_{22}(t) \propto t^{\beta}. \tag{37}$$

In the range $1 < \beta < 2$ the moments behave as

$$m_1(t) \propto t, \qquad \kappa_{11}(t) \propto t^{3-\beta}, \qquad \kappa_{22}(t) \propto t. \tag{38}$$

These behaviors are valid in their asymptotic trend if there exist time regimes for which the transition time pdf shows the power-law behavior $\psi(t) \propto t^{-1-\beta}$ for $0 < \beta < 2$. For $\beta > 2$ the breakthrough and dispersion behaviors are asymptotically Fickian. One could also expect that there exists a cut-off scale, seemingly linked to the largest velocity scale, beyond which the transition time pdf drops faster than a power-law. Such situations and the transitions from anomalous to normal transport behaviors have been investigated in Dentz et al (2004).

3 Numerical Random Walk Particle Tracking Methods

3.1 Classical Random Walks

The simplest random particle tracking algorithm to solve the ADE (5) is obtained by time discretization of the Langevin equation (9) relying on the Ito convention of the stochastic integral of $d\mathbf{x}/dt$,

$$\mathbf{x}(t+\Delta t) = \mathbf{x}(t) + \frac{\mathbf{u}[\mathbf{x}(t)]}{\phi[\mathbf{x}(t)]}\Delta t + \frac{\nabla\cdot\mathbf{D}[\mathbf{x}(t)]}{\phi[\mathbf{x}(t)]}\Delta t + \sqrt{\frac{2\mathbf{D}[\mathbf{x}(t)]\Delta t}{\phi[\mathbf{x}(t)]}}\cdot\mathbf{Z}(t), \qquad (39)$$

which yields an Euler scheme of the particle displacement. In the preceding equation, the time step is supposed to be discretized in increments dt. In the basic version, time steps are assumed to be constant. The $\mathbf{Z}(t)$ are independent random vectors of Gaussian components with zero mean, $\langle\mathbf{Z}(t)\rangle = \mathbf{0}$ and covariance $\langle Z_i(t)Z_j(t)\rangle = \delta_{ij}$. In practice, the random noise $\mathbf{Z}(t)$ can be replaced by any random vector with zero mean and unit variance. In the heterogeneous case, including media characterized by discontinuous properties, this classical formulation of RW has several drawbacks. Intuitively, one can anticipate spurious phenomena because of the Dirac delta function that appears in the evaluation of the gradient of discontinuous diffusivity. The first methods were based on reflection principles approximating the complete solution to the discontinuous interface, which can be obtained through the so-called method of images (Uffink, 1985; Semra et al, 1993; Kinzelbach and Uffink, 1991; Kinzelbach, 1988; Zimmermann et al, 2001; Hoteit et al, 2002a,b; Bechtold et al, 2011). When crossing the interface, random walkers are either reflected or transmitted. Starting from the higher dispersion side, random walkers are more likely reflected than dispersed, thus preventing from spurious accumulation of particles in the lower dispersive side. Thorough investigation of these approximations have been performed both theoretically by defining convergence conditions that should respect the proposed diffusive processes (LaBolle et al, 1998) and numerically by comparing them on different benchmarks (Salamon et al, 2006a; Lejay and Pichot, ????). Numerical studies point out the complexity of their implementation especially when coupling them with advanced discretization scheme for transport. Another drawback is that the basic algorithm leads to inefficient small spatial displacements in very low diffusion coefficient zones. The particles remain trapped in low diffusion zones, increasing the effective computational cost which is proportional to the number of time iterations. In the heterogeneous case, including media characterized by discontinuous properties, this classical formulation of RW has several drawbacks. Intuitively, one can anticipate spurious phenomena because of the Dirac delta function that appears in the evaluation of the gradient of discontinuous diffusivity. In the classical form of RW, accounting for these diffusivity discontinuities requires the implementation of quite complex "reflection" rules of the particles at the interface between two media

3.2 Fully coupled advection-dispersion-diffusion equation

Introducing advective and dispersive terms in the same equation raises specific numerical issues mostly linked to discontinuities in the dispersion gradient and to

the coupling between the first-order advective term and the second-order diffusive-dispersive term. Nonetheless, RW methods remain widely used because of their good numerical properties, irrespective the rate of advection to diffusion-dispersion and also because they are easily implemented. Time domain variants have drastically improved the performances of RW methods, especially when dealing with heterogeneous media. At the local scale, hydrodynamic dispersion is generally modeled as a Fickian diffusion with the diffusion-dispersion coefficient $\mathrm{D}(\mathbf{x})$ of equation (5) expressed as a tensor of components (Bear, 1973):

$$D_{ij} = (\alpha_T|\mathbf{v}| + d)\delta_{ij} + (\alpha_L - \alpha_T)\frac{v_i v_j}{|\mathbf{v}|} \tag{40}$$

where d is the diffusion coefficient, α_L and α_T are the longitudinal and transverse dispersivities, v_i is the velocity in direction x_i, $|\mathbf{v}|$ is the norm of the velocity, and δ_{ij} is the Kronecker symbol. Along the principal directions of dispersion, this expression simplifies into

$$D = \begin{bmatrix} d + \alpha_L|\mathbf{v}| & 0 & 0 \\ 0 & d + \alpha_T|\mathbf{v}| & 0 \\ 0 & 0 & d + \alpha_T|\mathbf{v}| \end{bmatrix} \tag{41}$$

where the first coordinate is taken along the direction given by the velocity and the two other directions are in the plane normal to the velocity.

Both the advective and dispersive terms require the determination of the velocity $\mathbf{v}$ at any location in the modeled domain, while Eulerian methods only require the knowledge of velocities at the scale of the mesh cell. When the velocity field has been obtained numerically from the discretization of the flow equation over a calculation grid, the velocity is expressed within each mesh cell by means of appropriate methods. If the numerical scheme is based on flux conservative Finite Element methods (e.g., Mixed Finite Element, Mixed Hybrid Finite Element) (Brezzi and Fortin, 1991; Hoteit et al, 2002a; Mosé et al, 1994; Pichot et al, 2010; Roberts and Thomas, 1991), the velocity is directly derived from a combination of the finite element basis functions (Hoteit et al, 2002b). With more standard Finite Element approaches, conservative velocity schemes can still be derived using flux-conserving sub-cell subdivisions (Cordes and Kinzelbach, 1992, 1996). For Finite Difference and Finite Volume schemes, velocities are most commonly calculated within mesh cells via multi-linear interpolations (linear along the different directions of the meshing) (Pollock, 1988; Maier and Bürger, 2013). In fact, only the linear interpolation scheme is flux-conservative. In the specific cases handling regular grids, the linear interpolation scheme can also be derived from the equivalence between Finite Volume methods and Mixed Hybrid Finite Element schemes (Chavent and Roberts, 1991). While mass-conservative transport schemes require flux-conservative schemes, they do not impose any condition to the transverse velocity across mesh faces that appear in general to be discontinuous. In association with the multi-linear interpolation schemes, shear deformation tends to accumulate at the edges of the mesh cell and is zero outside. This is a strong limitation when studying solute mixing mechanisms with geometrical and process-based analysis (Le Borgne et al, 2015). Alternative quadratic velocity interpolation schemes have been proposed to ensure non-slip boundary conditions at impervious limits (Nunes et al, 2015). Mass conservation conditions are no longer fulfilled locally but they

are globally, over cell facets. This type of interpolation scheme becomes appropriate in the presence of numerous no-flow boundary conditions (e.g. modeling transport at the pore scale).

While classical Eulerian schemes only need the expression of the dispersion tensor D (Zheng and Bennett, 2002), random walk methods also require the dispersion gradient (equation (5)), and thus the velocity gradient. This is an important specificity of RW methods that conditions the choice of both the numerical schemes and the implementation methods. The main difficulty stems from the discontinuity of the velocity gradient and hence of the dispersion gradient across cells. We first underline that the effect of the discontinuity at the cell facet is not systematically critical and is sometimes negligible compared with the other effects of transport. This is the case of heterogeneous permeability fields as the classical multi-Gaussian lognormal fields for which the transition between high and low flow zones remains gradual enough (Salamon et al, 2006b). While not fully tested, this point was hinted in previous studies (Tompson and Gelhar, 1990). In these conditions of heterogeneity, random walkers are much more dispersed by the velocity field and its gradient within the mesh cells than by discontinuities at the cell interfaces.

TDRW methods are in essence more appealing than RW because their random walkers stop at the interface before being transferred to neighboring cells (Bodin et al, 2007; Delay and Bodin, 2001). The travel time to the interface is drawn from exact or approximate analytical solutions to transport in homogeneous media. Developed first in one-dimensional media for simulating solute transport in fracture segments (Bodin et al, 2003; Painter and Cvetkovic, 2005), TDRW have been extended to multidimensional media (Bodin, 2015; Delay et al, 2002). When local analytical solutions of the travel time distribution can be obtained, TDRW methods are highly efficient to couple the advective and diffusive/dispersive transport processes. In the absence of local analytical solutions, alternative methods have been developed as a mix between "space-domain" random walk (classical random walk) and time-domain random walk and trying to combine both the spatial and temporal advantages. The constant displacement scheme consists in choosing a spatial scale Δx much smaller than the mesh scale l and deriving the time step Δt from the spatial scale divided the local velocity v (Beaudoin et al, 2007; Wen and Gomez-Hernandez, 1996; de Dreuzy et al, 2007): $\Delta t = \Delta x/v$. The classical space-domain random walk method is then run once for this time step Δt using both advection and dispersion mechanisms. The control by the velocity at the location of the random walker ensures that the mean displacement remains always equal to Δx. The characteristic number of steps taken within the mesh cell n can be obviously fixed by choosing $\Delta x = l/n$. The varying time step Δt according to the location in the domain maintains an even balance between accuracy and efficiency over the whole modeled domain. This method combines part of the efficiency of the TDRW method by fixing the mean displacement and the generality of the classical Space-Domain RW. It also fundamentally respects the flow structure within the mesh cell because the small displacements correctly follow the structure of flow lines in each cell. In classical implementations, dispersion discontinuities treated by the reflection method is again an issue. It could be solved by switching to TDRW when the random walker comes close enough to one of the cell facets. Close to cell corners, only the interface in the direction of the velocity could be considered.

3.3 Purely diffusive issues

In the case of purely diffusive issues as for Darcian fluid flow, we set$\mathbf{u}(\mathbf{x}) = 0$ in the ADE and rewrite the equation for the fluid pressure p (that replaces the notation c for this section) as:

$$\phi(\mathbf{x})\frac{\partial p(\mathbf{x},t)}{\partial t} = \nabla \cdot [D(\mathbf{x})\nabla p(\mathbf{x},t)] + S(\mathbf{x},t). \tag{42}$$

In the hydrogeology practice, or in the oil and gas industry, $D(\mathbf{x})$ is the diffusivity given by $D(\mathbf{x}) = \frac{k(\mathbf{x})}{\mu c_t}$, k is the permeability, μ is the fluid viscosity and c_t the total compressibility of the medium (rock plus fluid). A source term in the form $S(\mathbf{x},t)$ representing either sources and sinks, or boundaries has been added in the right hand side of the equation. Note that the equation can describe either tracer, thermal or pressure diffusion in a porous medium of weak compressibility. The linearity of this equation allows us to consider the cases where $S(\mathbf{x},t)$ is in the form $\delta(t)\delta(\mathbf{x}-\mathbf{x}_0)$. This means that we are interested in the Green's function of the previous equation. To go farther, a first step is to represent properly the heterogeneous (or fractured) medium by means of a geometrical meshing. In a second step, using an appropriate numerical scheme results in a discrete set of equations to be solved. Finally, RW methods are used to solve the equations and to glance at some information concealed in these equations.

3.3.1 Discretization of heterogeneous and fractured media

A discretization of the medium can be obtained via any available mesh builder handling triangular or quadrangular elements (or the corresponding elements in the three-dimensional case). In the case of bulk heterogeneities such as those mimicked by geostatistical random fields, any sufficiently refined meshing compared with the underlying correlation length will capture most of the heterogeneities (Fig. 1).

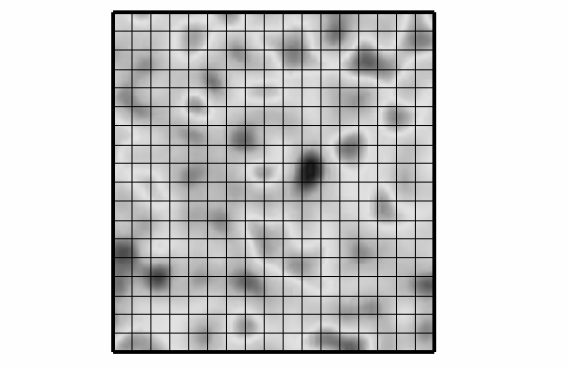

Fig. 1 An heterogeneous medium and the associated mesh

In the case of sharp heterogeneities enclosing discontinuities such as between different layers, it is assumed that the meshing follows the discontinuities. For

densely fractured media, building conform meshes (i.e., meshes not too much distorted) closely following the discrete network of fractures becomes almost infeasible (Fig. 2).

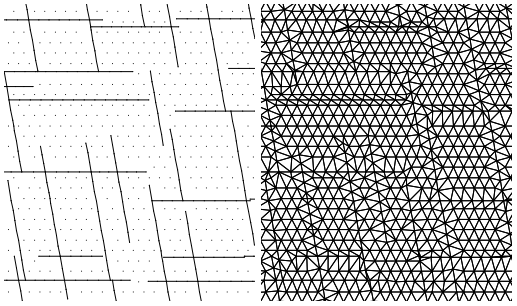

Fig. 2 A fractured unit cell and its triangulation

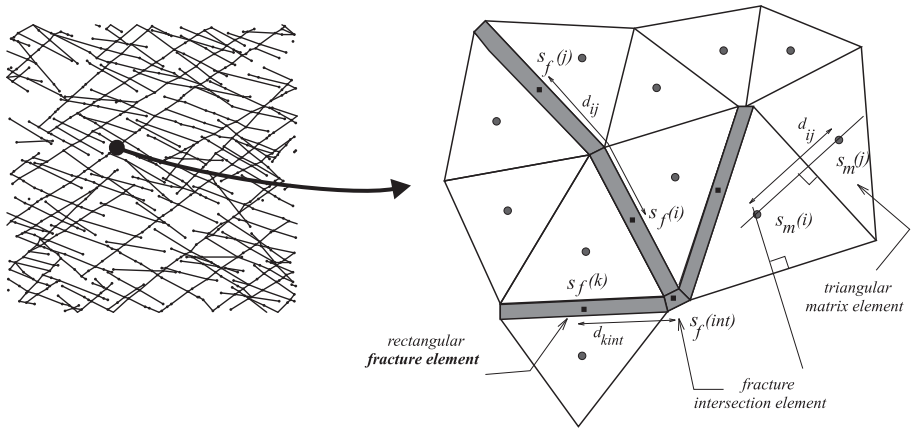

Fig. 3 Local zoom of the mesh

In a second step, the diffusion equation (42) can be discretized using Finite Volume or Finite Element methods, yielding usually a linear differential set of equations in the form of:

$$V_i \phi_i \frac{\partial p_i(t)}{\partial t} = \sum_{j \text{ neighbor } i} T_{ij}(p_j(t) - p_i(t)) + \int_{grid\ block\ i} S(\mathbf{x}, t) d\mathbf{x}. \tag{43}$$

Here, V_i denotes the volume of the i-th grid block. This step can result in additional geometrical constraints for the meshing that are beyond the scope of this study. Considering for illustration a Cartesian regular grid of spatial step Δx, using a Finite Volume approach, the discretized version of this equation in d dimensions

for each grid block of size $(\Delta x)^d$ can be written as:

$$(\Delta x)^d \phi_i \frac{\partial p_i(t)}{\partial t} = \sum_{j \text{ neighbor } i} T_{ij}(p_j(t) - p_i(t)) + \int_{grid\ block\ i} S(\mathbf{x}, t) d\mathbf{x}. \tag{44}$$

The summation is carried out with respect to index j labeling the nearest neighbors of the current grid block i.

It remains to define the so called transmissivities or inter block conductivities T_{ij} between two adjacent grid cells i and j with respect to the underlying heterogeneous map. A classical choice is the harmonic mean given by:

$$T_{ij} = 2\frac{D_i D_j (\Delta x)^{(d-2)}}{(D_i + D_j)} \tag{45}$$

where subscript i indicates that the values are evaluated at the center $\mathbf{x}_i$ of the i-th grid block. This provides a consistent discretization of (43) (McCarthy, 1990, 1991, 1993a,b). In the specific case of a fractured porous medium, mixing hydraulic properties of fractures and matrix, a different option is usually taken by assigning diffusion coefficient to meshes i in the form:

$$D_i = \left\{ \begin{array}{l} (\Delta x)^{(d-2)} D_m, \ \ if\ \mathbf{x}_i \in \Omega_m, \\ (\Delta x)^{(d-2)} D_f, \quad if\ \mathbf{x}_i \in \Omega_f. \end{array} \right\} \tag{46}$$

Here, Ω_f and Ω_m represent the fracture and the matrix domains, respectively. Using a sufficiently refined grid, allows relying upon standard Euler time discretization and associated solvers to produce accurate solutions of the discretized version of (43).

It is noteworthy that many discretization methods yield linear systems in the form of (43). Combining various mesh generators with compatible discretization schemes for the diffusion operator will always render the same general form of the discretized equations, the latter simply changing by the stencil of neighbor cells involved in each equation and the formulas of inter-block transmissivities (45). A rather complete analysis of this last issue can be found in Romeu and Noetinger (1995). It was observed that convergence to the solution of the continuous equations can be greatly accelerated according to the meshing and discrete scheme used. More recently, Wang et al (2014) and Qu et al (2014) detailed the local flow field close to adjacent corners of neighbor grid cells. These authors were able to justify the general power law averaging as the rule for generating inter-block coefficients by using the so called "finite analytic approach". It must be kept in mind that that with extreme contrasts of diffusion properties between cells, the standard choice of harmonic means (45) results in severe underestimations of the large scale diffusion, the harmonic mean being mainly controlled by the smallest value. In the case of percolation lattices involving highly contrasted properties, the percolation threshold might be artificially shifted. In the sequel, we will no longer come back to the choice of inter-block parameters even though it is an important feature for solving flow and transport equations.

3.4 Random walk methods for dual-porosity models

Fractured media are generally made of highly conductive fractures present at several scales and embedded in a low permeability matrix. This high contrast of properties led to the introduction of dual-porosity models where matrix and fractures are treated separately and coupled through an exchange term. These models have been used to simulate various processes, such as fluid flow (Barenblatt and Zheltov, 1960; Warren and Root, 1963), solute transport (Dershowitz and Miller, 1995; Cvetkovic et al, 2004), and electric current flow (Roubinet and Irving, 2014). They can also be associated with Dual-porosity models can also rely upon Discrete Fracture Networks (DFN) approaches to consider the geometrical complexity of realistic fracture networks (Cacas et al, 1990; Delorme et al, 2013a). In the purely diffusive case, these dual-porosity models can be ruled by the following equation:

$$\int_0^\infty d\tau[\phi_f V_f \delta(t-\tau)+\phi_m V_m f(t-\tau)]\frac{\partial p(\mathbf{x},\tau)}{\partial \tau} = \nabla\cdot[D(\mathbf{x})\nabla p(\mathbf{x},t)]+S(\mathbf{x},t). \quad (47)$$

Here, V_f and V_m denote the volume fractions of the fractures and the matrix, respectively, and ϕ_f and ϕ_m are the associated porosity.

The Laplace transform of eq (47) yields:

$$[\phi_f V_f + \phi_m V_m f(s)][s\,p(\mathbf{x},s) - p(\mathbf{x},t=0)] = \nabla\cdot[D(\mathbf{x})\nabla p(\mathbf{x},s)] + S(\mathbf{x},s). \quad (48)$$

In some dual-porosity models, RW methods have been used for: (i) up-scaling the transfer properties required to describe averaged fracture-matrix interactions, (ii) directly solving the considered flow or/and transport problem, and (iii) evaluating flow or/and transport effective properties. In this section, we describe a few of these applications distinguishing the dual-porosity models based on a continuous representation of the fractures (section 3.4.1) from models based on an explicit representation of the DFN (section 3.4.2).

3.4.1 Up-scaling DFN to continuum dual-porosity models

Solving fluid flow in fractured porous media can be carried out by resorting to a continuous dual-porosity model, such as the one described in Appendix B. The model description handled in the present study lets appear transfer functions and coefficients between fracture and matrix continua, denoted $f(t)$ and λ, respectively. Although these functions and coefficients can be determined analytically for simple cases (expressions (70)-(71)), a numerical evaluation is required for the complex cases. In this context, Noetinger and Estebenet (2000), Noetinger et al (2001a,b) and Landereau et al (2001) applied directly a TDRW method (named CTRW in their papers) to determine these transfer parameters. The key observation of Noetinger and Estebenet (2000) and Noetinger et al (2001a) is that $f(t)$ can be interpreted as the probability density function (pdf) of the first exit time of a particle initially launched from a random location in the matrix, then undergoing a random motion in the matrix and finally exiting toward the fracture domain at the matrix boundary. This function $f(t)$ might also be identified as the local memory introduced for general processes hosting mobile-immobile physical and chemical interactions (Carrera et al, 1998; Willmann et al, 2008). It can be verified explicitely on the few analytical solutions of $f(s)$ (Appendix B) that the transfer

function can be developed as a power serie of s (Noetinger and Estebenet, 2000; Noetinger et al, 2001a):

$$f(s) = 1 - \frac{\phi_m V_m}{\lambda} s + ... \tag{49}$$

Recasting the equation in the real domain yields $\langle t \rangle = \int_0^{+\infty} t f(t) dt = \frac{\phi_m V_m}{\lambda}$. Therefore, the mean residence time of random walkers in the matrix is directly related to the transfer coefficient introduced in dual-porosity models. It can be shown mathematically that the λ coefficient arising from this definition exactly coincides with the coefficient obtained from large scale averaging or homogenization theory (Noetinger et al, 2001b). These considerations result in the following algorithm that provides a full determination of the exchange function $f(t)$ as well as the parameter λ. Without loss of generality, we assume $\phi_m = 1$. It is assumed that the matrix was meshed and that a finite volume scheme led to a discretized set of equations having the form of 43. We introduce the notations: $B_i = \sum_{[ij]} T_{ij}$ and $w_{ij} = \frac{T_{ij}}{B_i}$ The following algorithm can be easily implemented:

1. Choose the number N of independent particles.
2. To start the i-th particle, choose one matrix node j_i with a probability proportional to the volume of the associated grid block, k=1.
3. While the particle has not left the matrix, at step k of the algorithm, move the particle from site "i" to its nearest neighbor site "j", with a probability equal to w_{ij}
4. Update the time counter with the relation:

$$t_k = t_{k-1} - \frac{V_i}{B_i} Log(rand).$$

   Here, *rand* stands for a random number picked from a uniform distribution over $[0, 1]$.
5. If at iteration k the particle enters a grid block belonging to the fracture region at iteration k, store the exit time $t^i = t_k$ of the current particle i and launch the i+1 th particle.
6. Store the N independent exit times $t^{(1)}$,..., $t^{(N)}$.
7. End.

It is then easy to obtain the histogram of the distribution yielding $f(t)$. The quantity λ can be estimated by means of the relation

$$\lambda = \frac{V_m}{\langle t_{mf} \rangle} \simeq \frac{V_m}{\frac{1}{N} \sum_{i=1}^{N} t^{(i)}}.$$

The above algorithm, which returns a direct determination of the complete exchange function, is very fast and efficient because there is no need of iterations (particle motions) in the fractures. It was successfully tested on simple geometries consisting of for stratified media, or spherical matrix blocks and provided good comparison with the corresponding analytical determinations of both $f(t)$ and λ (Noetinger and Estebenet, 2000; Noetinger et al, 2001b,a). In addition in these papers, it was shown that this exchange function $f(t)$ is closely related to the time autocorrelation function of $I_f(t)$. Here, the fracture indicator function is defined as $I_f(t) = 1$ if the particle in the fracture at time t, 0 else. This corresponds to the curve labelled by FMF in (Fig. 4).

Several tests on simple DFN's with some randomness in the fracture characteristics were also carried out (Fig. 4). The residence time distribution $f(t)$ obtained by TDRW compared very well with the corresponding finite volume solutions. These solutions were obtained by solving the relaxation problem given in the appendix 67 that is closely related to determination of the fisrt exit time distribution $f(t)$.

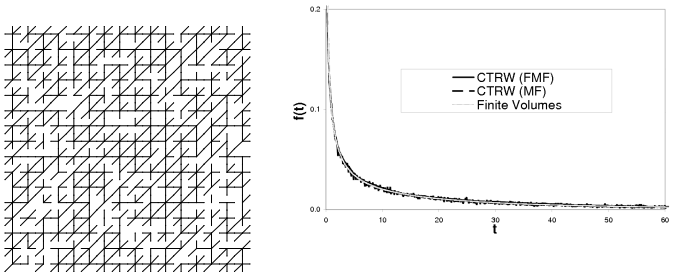

Fig. 4 Left: a fractured medium. Right: transfer function computed by TDRW and by finite differences.

It remains to characterize transfer functions for complex DFN. Finding generic analytical forms generalizing the known analytical forms given in appendix B (69,70, 71) and able to account for very wide distributions of matrix block size remains to be done. At short times, corresponding to large Laplace parameter s, the function $f(t)$ is sensitive to the ratio of the fracture surface to total volume. At larger times, $f(t)$ samples the whole block size distribution, making that some fractal and thus "anomalous" power law behavior may be anticipated. This could lead in the real time domain to anomalous transfer kernels equivalent to fractional derivatives (Néel et al, 2011, 2014). There is no doubt that the TDRW method depicted above would be useful to feed the investigations with numerical results. As an illustration the method was implemented to estimate some properties of fractured medium constructed with percolation lattices. Fig. 5 shows a realization of a percolation lattice with a proportion $p = 0.57$ of active fractures. In Fig. 6, we plotted the dependence on $p - p_c$ of the mean residence time in the matrix (with diffusivity equal to one) with respect to the proportion of active fractures. The flexibility of the TDRW approach allows to compute several mean residence times of interest, that depend on the fracture sub-network that is retained to decide to stop the particle's motion in the algorithm above (the reader can remark that any arbitrary stopping criterion can be imposed in the algorithm above). This freedom was used to study the residence time distribution computed once retaining the whole fracture network (the basic algorithm), or only the connected cluster, or only the resulting backbone, neglecting dead ends. In order to account for finite clusters, particles attaining an isolated cluster, are instantaneously released at a random location in a matrix mesh bounding this cluster (so called "speed on isolated clusters") and may continue their diffusive motion before attaining the sub-network of interest at which the exit time t_i is stored. Then average residence times can be evaluated depending on the proportion p of active fractures.

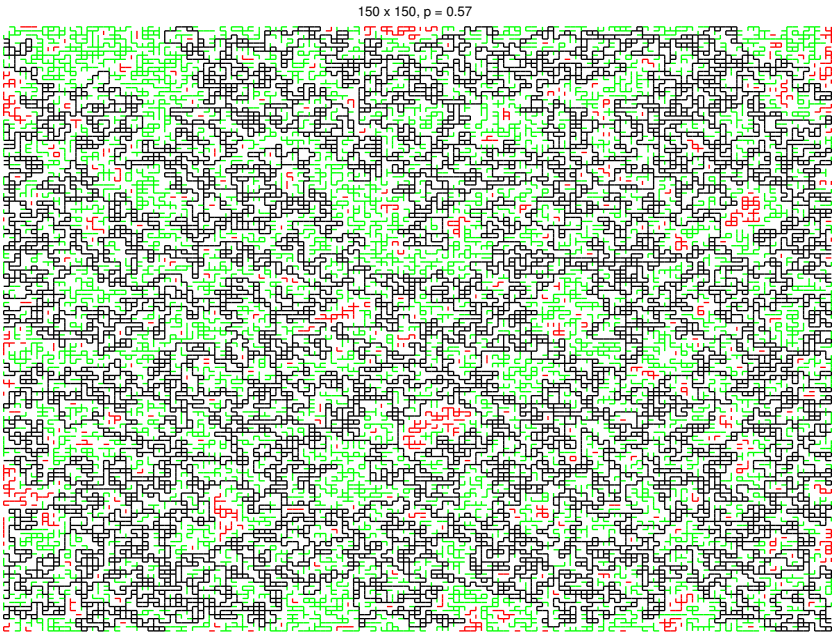

Fig. 5 A bond percolation network at proportion $p = 0.57$ of active fractures, red = isolated clusters, black = backbone, green= dead-ends

A set different curves corresponding to different mean residence times $\langle t \rangle$ is obtained. Each curve depends on the fracture subnetwork that was kept, i.e., all the fractures including non-relevant isolated clusters (red dots), or only the percolation backbone (black triangles) corresponding to the extreme cases. Intermediate curves correspond to different treatments of the remaining finite clusters. Notably, keeping the whole set of fractures (red dots) in Fig. 6 does not lead to any critical divergence of the mean residence time close to p_c ($p_c = 0.5$ in the case of a 2D bond square lattice). Further studies should be carried out to obtain a better characterization of the associated critical exponents. This result illustrates that even starting from the same DFN, exchange coefficients may be process dependent, depending on the role of finite clusters or dead-ends in the transport process under consideration.

It can be mentioned that random walk methods have also been used in continuous dual-porosity models to directly model transport in fractured porous media (Liu et al, 2000; Pan and Bodvarsson, 2002). In these studies, advection-dispersion equations were considered in both the fracture and matrix continua, and the probability of transfer between these two continua was defined analytically.

3.4.2 Random walk simulations on discrete fracture networks accounting for the matrix

In the preceding section, it was shown that the transfer function $f(t)$ could be determined efficiently using TDRW. Once $f(t)$ is found applications can be envisioned by using the continuous double porosity equations (60) or the alternative form (63). Another option is to keep the details of the DFN topology explicitly,

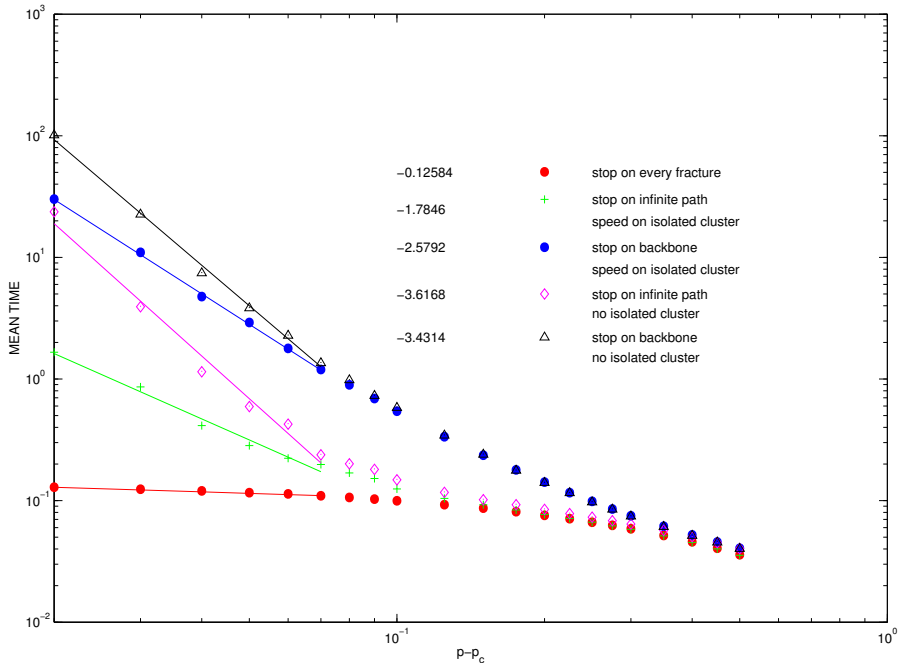

Fig. 6 Exchange coefficient computed for the percolation network as a function of $p - p_c$. The indicated numbers correspond to the estimated slopes of the apparent scaling laws in this Log Log representation.

without keeping an expensive explicit meshing of the fractures. In two dimensions, the DFN is represented by means of a resistor/capacitor network with pressure unknowns located only at the intersections of the fractures. This class of models are called pipe network models. Chang and Yortsos (1990) and Acuna and Yortsos (1995) carried out simulations of pressure transient (well tests) in this way using two-dimensional DFN close to the percolation threshold. The components of flow between matrix and fractures were neglected, corresponding to studying an impervious matrix. A three-dimensional generalization of this pipe network approach including these components was proposed by Noetinger and Jarrige (2012) and Noetinger (2015). The main difficulty is that in 3 d, intersections between fractures are segments, so describing pressure profiles at these intersections involves many degrees of freedom. By introducing the set of fracture intersections labeled by j, and denoting p_j as the average pressure on the j-th intersection, it is possible to derive the following set of equations that corresponds to a lowest order approximation:

$$\forall i = 1, N_{\cap}, \quad \sum_{j \in J(i)} K_{ij}^{11}(V_f + V_m f(s))[sp_j(s) - p_j(t=0)] = \sum_{j \in J(i)} V_f T_{ij}^{11} p_j(s) \quad (50)$$

To simplify notations, both matrix and fracture porosity are here equal to unity. The quantities K_{ij}^{11} and T_{ij}^{11} depend explicitly on the shape of the fractures and can be determined with fast algorithms (Khvoenkova and Delorme, 2011; Delorme

et al, 2013b). One can note that the number of unknowns corresponds to the number of intersections between fractures, so the method allows treating large DFN's. If a better accuracy is needed, one can increase the order of the approximation, but the number of unknown remains still Noetinger and Jarrige (2012) and Noetinger (2015). The set of equations 50 has the same form that a discrete form of the set of equations (63) that can be solved using TDRW with trapping as introduced by Dentz et al (2012), equations (26), (29), (30) and (31) of their contribution. Identification is obtained by stating

$$(V_f + V_m f(s)) = \frac{1}{\mu(\mathbf{x}, s)} \tag{51}$$

where $\mu(\mathbf{x}, s)$ is the local memory function introduced in Dentz et al (2012). To summarize, one can state that TDRW is useful to both:

- determine $f(t)$ using random walkers in the matrix only, the DFN acting as a boundary
- once $f(t)$ properly known, solving equations (50) to up-scale the DFN in order to parameterize a continuous double porosity model useful for engineering applications.

TDRW methods associated with an explicit representation of the DFN have also been used to model transport processes in fractured media Geiger et al (2010). Some models only consider advective displacement in the fractures with the aim of studying hydrodynamic dispersion in two-dimensional heterogeneous percolation networks (Rivard and Delay, 2004). In these studies, binary and log-normally distributed hydraulic conductivity fields are considered, and the impact of this heterogeneity on the longitudinal dispersion coefficient is analyzed at the percolation threshold. In other models, advection-diffusion mechanisms in the fractures and pure diffusion in the matrix are considered, with sometimes a mesh-free representation of the matrix. This dual-porosity formulation reduces the numerical cost and the algorithm complexity related to the meshing step of each simulation. With these techniques, particles only move in the fractures and their diffusion into the surrounding matrix is considered via an additional retardation time (Cvetkovic et al, 2004; Dershowitz and Miller, 1995; Roubinet et al, 2010). When derived from analytical solutions, this retardation time relies on specfic physical and geometrical assumptions. For example, Dershowitz and Miller (1995) consider a pure-diffusion equation in matrix blocks of regular shape. In Cvetkovic et al (2004), retention models based on analytical solutions of fracture-matrix systems (e.g., Tang et al (1981)) are employed under the assumption that the matrix surrounding each fracture is infinite yielding no limitation of matrix diffusion by nearby fractures. To overcome this restrictive assumption, Roubinet et al (2010) add the possibility for each particle to transfer from one fracture to another by diffusion through the matrix blocks. The method is applicable to heterogeneous fractured porous media without constraint on the matrix block geometry or network density.

The numerical methods previously described have been used to evaluate up-scaled transport properties and to analyze the impact of structural heterogeneity at the large-scale on the behavior of transport in fractured media. In Cvetkovic et al (2004), Painter and Cvetkovic (2005), and Painter et al (2008), up-scaled transport properties are first evaluated over small discrete fracture networks, and then used to perform large-scale simulations. This efficient two-step method has

been applied to the Äspö Hard Rock Laboratory in Sweden (Cvetkovic et al, 2004; Painter and Cvetkovic, 2005) and has been extended by introducing first-order (kinetics) solute transformations (Painter et al, 2008). Other RW methods associated with a DFN representation have helped to understand the impact of the DFN heterogeneity on large-scale effective transport properties. More precisely, Liu et al (2007) aimed their study at the dependence with the space scale of the effective matrix diffusion coefficient deduced from field tracer experiments. This scale effect has been observed in numerous characterization studies of fractured rocks, and the numerical simulations conducted in Liu et al (2007) showed that this effect was related to the DFN heterogeneity. The impact of DFN heterogeneity has also been studied in Roubinet et al (2013) by way of numerical transport simulations conducted over synthetic fracture networks with large ranges of hydraulic properties and wide distributions of matrix block size.

3.5 Measuring Mixing Properties From Random Walk Simulations

Mixing is one of the key mechanisms of interest when studying transport and reaction phenomena in heterogeneous porous and fractured media (Kitanidis, 1994; Dentz et al, 2011). While dispersion measures the spatial extent of conveyed plumes, mixing quantifies the distribution of concentration of dissolved chemical species in the fluid phase (Le Borgne et al, 2015). Therefore, mixing measures both the dilution of plume in the resident fluid and the probability of dissolved reactive species to meet and react (de Simoni et al, 2005). Different mixing measures have been proposed including the dilution index (Kitanidis, 1994), the intensity of segregation (Danckwerts, 1952) and the scalar dissipation rate (Ottino, 1989). The latter measures the rate at which concentration gradients are dissipated under the combined action of advection and diffusion. It can be directly translated into an effective reaction rate when fast reactions are considered (Le Borgne et al, 2010; de Simoni et al, 2005).

Numerical particle tracking methods are particularly useful to investigate dispersion and mixing as they avoid numerical dispersion. Nevertheless, handling a finite set of particles is typically faced with significant noise and imprecisions in the calculation of concentration gradients, whose reduction requires a large density of particles. This is an issue when estimating scalar dissipation rates that depend on the concentration gradients according to

$$\chi(t) = \int dx D \left[\nabla c\right]^2 , \tag{52}$$

where D is the local diffusion coefficient and c is the local concentration. This local value of $D\left[\nabla c\right]^2$ is also useful as the interpretation of the sensistivity of large scale parameters to local heterogeneities (Noetinger, 2013). This measures of mixing is significantly affected by errors in concentration gradients since the latter appear squared in the measure. However, for finite time injection conditions, i.e. when no additional solute is injected in the domain when scalar dissipation is measured, it can be shown that the scalar dissipation rate is directly linked to the derivative with respect to time of the squared concentration as,

$$\chi(t) = -\frac{1}{2}\frac{d}{dt}\int dx\, c^2. \tag{53}$$

The expression shows that the scalar dissipation rate is a measure of the decay of concentration variance as the transported plume is diluted in the resident fluid. As illustrated in Fig. 7 and discussed in Le Borgne et al (2010), it comes out that expression (53) is far less sensitive to numerical noise than the classical expression of the scalar dissipation rate (equation (52)) because it does not require evaluating concentration gradients. With measure based on (53), mixing can be evaluated efficiently from random walk particle tracking simulation in heterogeneous media (Le Borgne et al, 2010). As illustrated in Fig. 7d, heterogeneity in permeability is found to induce temporal scaling effects of the mixing rates that distinguish from those expected for homogeneous media. This phenomenon can be explained by an enhancement of diffusion due to the stretching of the solute plume by velocity gradients (Le Borgne et al, 2013).

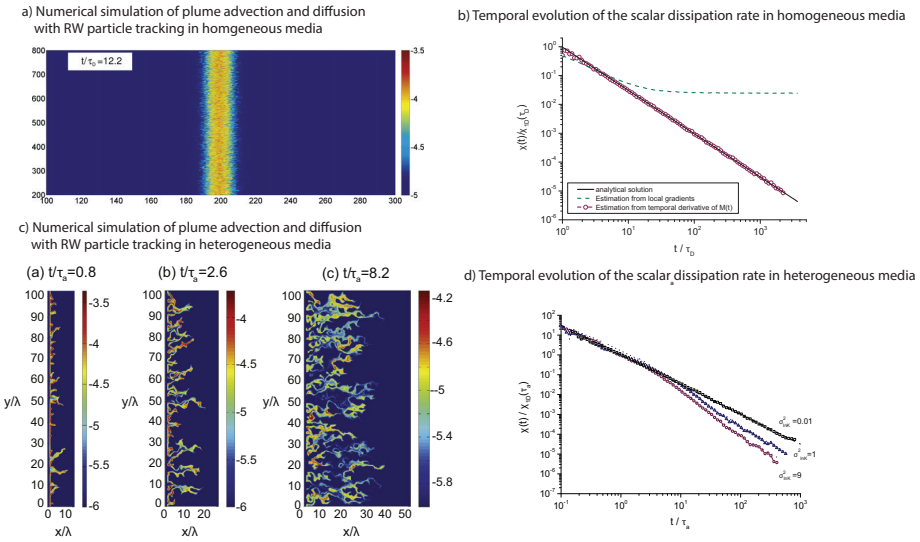

Fig. 7 a. Numerical simulation of the transport of a line of tracer in a homogeneous media under advection and diffusion with particle tracking. τ_D is the characteristic diffusion time over a pixel of size Δx, $\tau_D = \Delta_x^2/D$ b. Estimation of the scalar dissipation rate from the local concentration gradients (52) and from the local concentration squared $M(t) = \int dx c^2$ (53). The latter compared much better than the former to the analytical solution for a homogeneous media $\chi_{1D}(t) = \frac{C_0^2 L_y t^{-3/2}}{8\sqrt{2\pi D}}$. c. Numerical simulation of the transport of a line of tracer in a heterogeneous media under advection and diffusion with particle tracking. d. Temporal evolution of scalar dissipation rates estimated for different permeability field variances. Heterogeneity in permeability affects the temporal scaling of the scalar dissipation rate and thus the global mixing rate. Adapted from Le Borgne et al (2010).

4 Application from pore to field scale

4.1 Effective flow and transport parameters

A direct application of RW methods for diffusion problem is the determination of effective conductivity (or diffusivity) of heterogeneous media, by means of the Einstein relation bridging the mean square displacement to the effective diffusion coefficient of the handled equation (Einstein, 1956):

$$R^2(t) = \langle (x(t) - x(t=0))^2 \rangle = 2dD(t)t, \tag{54}$$

where d is the dimensionality of the system and $D(t)$ denotes the scaling coefficient of the diffusion equation under consideration (diffusion, diffusivity or conductivity). In the case of bulk heterogeneous media, it is possible to show that the convergence of $D(t)$ to its asymptotic value D_{eff} is reached once $R^2(t) \gg l_c$, where l_c is the permeability correlation length (Noetinger and Gautier, 1998). Physical considerations show that at short times, $R^2(t) \sim \bar{D}t$ where $\bar{D}$ denotes the average diffusivity, because the diffusive particles sample local homogeneous regions of size l_c. The cross-over between both regimes can provide information on the REV size. This technique has also been often used to analyze binary media, for instance that obtained from X-ray tomographic imaging (e.g. Gouze and Luquot (2011)). The effective diffusion and tortuosity can be obtained from the asymptotic regime but but the surface to volume ratio is also obtained from the transient regime (Sen et al, 1994; Sen, 2003, 2004). RW calculations inferring the effective properties at the sample scale of binary images of porous media can be efficiently performed using a TDRW approach. The regular lattice over which particles are moved by jumps of prescribed sizes is mapped onto the image voxels. Calculation of D_{eff} from binarized media can be performed by solving a boundary value problem mimicking a diffusion experiment where the particles are initially located at one boundary of the medium and the first passage time monitored at the opposite boundary. A more efficient method is to distribute randomly the particle in the pore space (initial value problem) and apply directly (54) to measure the evolution of $D(t)$ in time t and obtain D_{eff} from the asymptotic behavior of $D(t)$. Practically, it may become difficult to observe the asymptotic behavior of $D(t)$ because the sample does not enclose heterogeneity of finite scale and/or because calculations were stopped too early. For example, particles might spend a huge time to reach tiny connected paths in binary media close to the percolation threshold, making that anomalous diffusion occurs (Sahimi, 2011; Redner, 1989).

RW methods have also been employed to calculate the effective dispersion of binarized porous media by solving (5) in which a steady-state velocity field is obtained solving the Navier-Stokes equations using a classical Finite Volume approach. This approach was initiated by Salles et al (1993). The geometry of the simulations as well as the boundary and initial conditions are generally chosen to mimic laboratory tracer tests experiments through core samples. The settings are usually of "permeameter" type with a passive tracer injected at one side of the core and the tracer breakthrough curve (BTC) monitored at the opposite side. A pulse injection is usually mimicked in the numerical simulation instead of continuous injections of actual experiments because the pulse fasten computations (less particles in the system). In general, the size of the domain is limited by the computational effort needed to solve the Navier-Stokes equations; the current pattern being

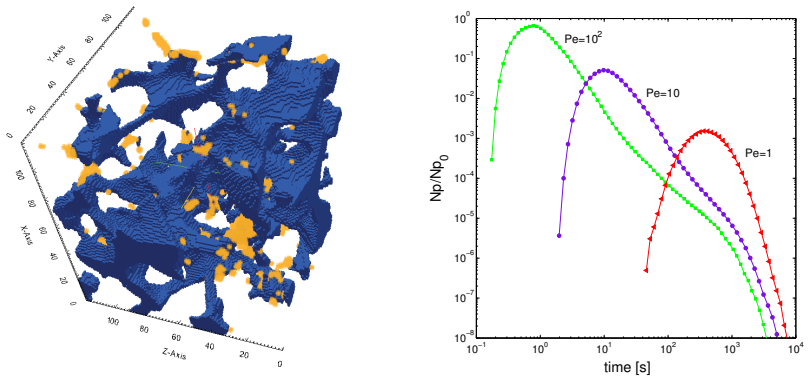

Fig. 8 Left: three-dimensional visualization of the pore network (blue) and the connected microporosity (yellow) for a sub-volume of 120^3 voxels of the ($0.8\ mm^3$) Berea sandstone sample studied by Gjetvaj et al (2015). Right: BTCs for pore-scale mobile-immobile transport through the Berea sample for different values of the Peclet number computed by TDRW.

three dimensional lattices of 300^3 to 1000^3 nodes that correspond to millimeter-sized rock samples. Nevertheless, this approach relying upon TDRW calculations remains appealing regarding the studies on the relationships between flow field properties and solute dispersion evidenced by markedly non-Fickian breakthrough curves. Bijeljic et al (2013a,b) studied the dispersion in carbonate and sandstone rock samples using binarized images of X-ray tomography. They simulated transport in moving particles by advection along streamlines (previously computed from the flow field) and using a classical RW with jumps of constant time step to simulate molecular diffusion. The authors characterized the heterogeneity of the porous medium as the distribution of pore throat size and showed that an asymptotic diffusion was reached after the particles had visited many throats. Conversely, Gjetvaj et al (2015) investigated the origin of non-Fickian transport using the Berea sandstone containing a small fraction of micro-porous cement with pore size below the resolution of X-ray micro-tomography (Fig. 8). The authors showed that the micro-porous phase was fairly well depicted as an immobile diffusive domain while the solute transport in the macro-porosity taken as a mobile domain was solved as a combination of Navier-Stokes and diffusion equations. Solute motion in the modeled sample was simulated by TDRW and showed that breakthrough curves exhibited non-Fickian diffusion processes stemming from the heterogeneity of the flow field and the diffusion into the micro-porosity. Finally, the authors proposed an up-scaled one-dimensional model calculating transition times of particles conditioned by (time)truncated power law distributions representing the effects of both the flow field heterogeneity and trapping plus diffusion mechanisms in the micro-porosity.

McCarthy (1990, 1991, 1993a,b) was the first author carrying out TDRW calculations for the purpose of up-scaling hydraulic-conductivities. Latter, random walk methods were also used to up-scale the transport properties of heterogeneous porous media at diverse scales. For example, at the large scale, heterogeneity of permeability has been represented by a lognormal exponentially correlated distribution and the flow equation was discretized and solved with a Finite Difference

scheme (de Dreuzy et al, 2007; Beaudoin et al, 2010; Beaudoin and de Dreuzy, 2013). Then, the effective longitudinal and transversal dispersions were inferred by way of two-dimensional (Beaudoin et al, 2010; de Dreuzy et al, 2007) and three-dimensional (Beaudoin and de Dreuzy, 2013) TDRW calculations. An additional advantage of TDRW methods for advective-dispersive transport in fractured networks is their capability to separate the transport within the fractures from mechanisms at fracture intersections. Different assumptions can be applied at the fracture intersections from complete mixing to streamline routing (Berkowitz et al, 1994; Kosakowski and Berkowitz, 1999; Park et al, 2003), resulting in markedly different solute mixing behaviors at the network scale (Bruderer and Bernabé, 2001; de Dreuzy et al, 2001; Park et al, 2001).

4.2 Interpretation of solute transport experiments

At the laboratory scale, CTRW has been used to interpret transport experiments set up as either saturated and unsaturated flow cells conveying sorbing and non-sorbing solutes (Hatano and Hatano, 1998; Berkowitz et al, 2000; Bromly and Hinz, 2004; Cortis and Berkowitz, 2004), or a single fracture in granitic core samples percolated with non-sorbing tracers (Jimenez-Hornero et al, 2005).

Random Walk approaches have also been used to interpret non-Fickian diffusion evidenced by in-situ field tracer test experiments. One of the most common evidence of non-Fickian transport processes is the flat tailing of breakthrough curves at long travel times that marks slow release of weak solute concentrations (Fig. 9) (Haggerty et al, 2000; Berkowitz et al, 2006). This tailing behavior holds information about the underlying processes triggering non-Fickian transport.

For example, matrix diffusion is known to impart strong tailings. As explained in section 2, this problem can be modeled in adding to the Fickian ADE a sink-source term accounting for mass transfers between the mobile domain and the matrix (immobile domain) where diffusion dominates:

$$\phi(\mathbf{x})\frac{\partial c(\mathbf{x},t)}{\partial t} - \nabla\cdot[\mathbf{D}\nabla c(\mathbf{x},t) + \mathbf{v}c(\mathbf{x},t)] + S(\mathbf{x},t) = 0 \tag{55}$$

with

$$S(\mathbf{x},t) = \phi'(\mathbf{x})\frac{\partial}{\partial t}\int dt'\, M(\mathbf{x},t-t')\, c(\mathbf{x},t'), \tag{56}$$

where ϕ and ϕ' denote the porosity in the mobile and immobile domain respectively and M is the (eventually spatially distributed) memory function that contains all the information on the geometry, the volume fraction of the immobile domain, and its accessibility to tracer particles conveyed in the mobile domain.

Various formulation of this sink-source term $S(\mathbf{x},t)$ were given to model the multi-rate nature of mobile-immobile mass exchanges that even occur in homogeneous media with simple geometries (Haggerty and Gorelick, 1995; Carrera et al, 1998; Haggerty et al, 2000). For these simple configurations, the tailing of breakthrough curves drops as $c(t) \sim t^{-1.5}$.

However, natural systems often display widespread clusters of matrix with heterogeneous diffusion properties (see for example Fig. 8) from which diverse tailing effects can be expected. Field observations report on power law distributions

of large travel times of concentrations $c(t) \sim t^{-1-\beta}$, with power law exponents spanning the wide range $0 < \beta < 2$ (Haggerty et al, 2000). Another form of tailing is the one displaying several slopes like the tracer tests by injection-withdrawal in a single well ("push-pull" experiment) discussed in Gouze et al (2008a).

Gouze et al (2008b) computed the memory function $M(t)$ associated with solute transport simulated over X-ray micro-tomography images. As a first step, the authors processed the images to delineate the interface between the mobile immobile domains and to evaluate the diffusion coefficient distribution within the immobile domain. In a second step, they computed the memory function by way of a constant time step RW approach. The calculation was implemented as follows. N random walkers uniformly distributed over the mobile-immobile interface are released at the initial time (t=0). The diffusion equation is solved by a discretized version of the Langevin equation (see (39)) and a specific procedure is applied to determine the trajectory of the random walkers through the heterogeneous pixelized matrix at each time increment. For $t > 0$, the mobile-immobile interface is considered as an absorbing boundary, making that random walkers jumping from the immobile domain toward the mobile domain are removed. The total number of random walkers inside the immobile domain $N'(t)$ is recorded until the last particle leaves the immobile domain. The authors showed that the memory function $M(t)$ could be obtained from the ratio $N'(t)/N$. Finally, Gouze et al (2008a) compared the memory function computed at the pore scale on X-ray micro-tomography images of core samples to the memory function of field scale tracer tests experiments in the limestone (Gouze et al, 2008a) where the core samples had been imaged. The authors concluded that the non-Fickian dispersion measured at the meter scale (field experiment) was fairly well explained by the microscale diffusion processes in the rock matrix of cores.

Le Borgne and Gouze (2008) developed a specific model to explain the two-slope tailing breakthrough curves discussed in Gouze et al (2008a) about push-pull tracer tests in a single well. The *op. cit.* authors implemented a continuous time random walk (CTRW) similar to that presented in section 2.2 and handling a transition time distribution $\psi(t)$ of dual-slope power law type. The best fit of tracer test data was obtained with a transitional regime modeled by $\psi(t) \propto t^{-2}$ and the asymptotic regime of a homogeneous dual-porosity model (i.e. $\psi(t) \propto t^{-1.5}$).

As alternative interpretations to the heterogeneous diffusion modeled by multi-rate mass transfer or CTRW, diverse processes have been evoked to explain the exponents of power-law travel time distributions, including heterogeneous advection in independent flow paths modeled by stochastic stream tube approaches (Becker and Shapiro, 2003). Both multi-rate mass transfer and heterogeneous advection have been modeled by random walk approaches (Kang et al, 2015; Gjetvaj et al, 2015).

In the CTRW framework, a power law tailing $c(t) \sim t^{-1-\beta}$ can be modeled by considering a transition time pdf in the form of $\psi(t) \sim t^{-1-\beta}$. The evolution toward Fickian transport can be modeled by including a cut-off threshold in the above power law (Dentz et al, 2004). While CTRW approaches generally describe non-Fickian transport as series of uncorrelated particle motions of very large durations, stochastic stream tube approaches (Becker and Shapiro, 2003) assume that particle velocities are constant along each streamline (particle jumps are therefore correlated) but differ from a streamline to one another. Becker and Shapiro (2003) have reported that this process led to the tailing of breakthrough curves obeying

the relation $c(t) \sim t^{-2}$ under convergent tracer test conditions. Different exponents were found for "push-pull" test depending on the duration of the injection (push) step. Kang et al (2015) showed that both non-Fickian transport and heterogeneous advection could be modeled by CTRW algorithm with correlated transition times, whose correlation are varied from zero to represent non-Fickian transport, to infinity to represent heterogeneous advection. It is not always straightforward to decipher and separate the role of diffusive and advective processes as they can lead to similar power law exponents of breakthrough tails. As shown by Kang et al (2015), this uncertainty on process controlling "anomalous" transport can be resolved by combining tracer test experiments under different conditions, including cross-borehole and push-pull tests. Cross borehole tests are more sensitive to heterogeneous advection, while push pull tests are more sensitive to diffusive mechanisms (Fig. 9).

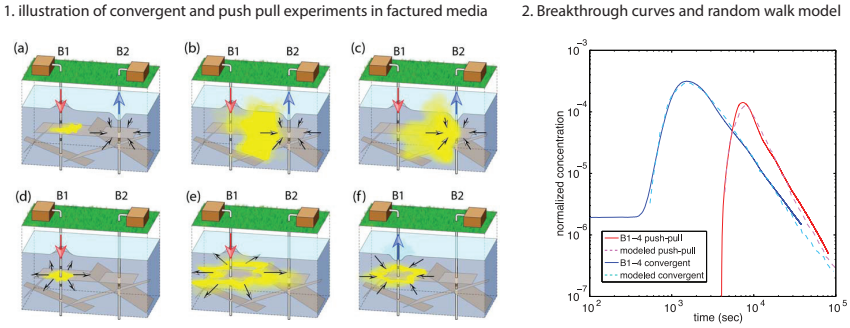

Fig. 9 1. Illustration of convergent and push pull tracer experiments in fractured media, from Kang et al (2015), 2. Breakthrough curves measured at the Ploemeur site (H+ network) under convergent and push pull conditions, and random walk modeling (dashed lines) with a Markov Chain CTRW model, from Kang et al (2015).

4.3 Modeling of transport processes under ambient conditions

RW methods have also been used to improve our understanding of transport processes under ambient conditions in natural environments. A lot of these studies have been conducted on fractured rocks using TDRW methods within the framework of discrete dual-porosity representations of the medium. Some of these models are described in section 3.4.2 and have been used, for example, to describe the migration of radionuclides through fractured rocks at the Äspö Hard Rock Laboratory in Sweden (Cvetkovic et al, 2004) and the Topopah Spring welded unit in Yucca Mountain (Pan and Bodvarsson, 2002). Other applications target the fractured Laxemar site in Sweden, which is part of the candidate repositories of spent nuclear fuel (Cvetkovic and Frampton, 2012), and the Kamaiski experimental mine site in Japan (Dershowitz and Miller, 1995).

Transport processes have also been modeled with RW methods in the context of colloidal transport in a shear zone (Kosakowski, 2004), for identifying chemical retention times in water catchments (Scher et al, 2002b), and for solute transport in rivers (Boano et al, 2007). CTRW has also been used to interpret the

observations made in a heterogeneous alluvial aquifer at the Macrodispersion Experiment (MADE) site of the Columbus Air Force Base (Mississippi) (Berkowitz and Scher, 1998) and in a fractured till located on the island of Funen (Denmark) (Kosakowski et al, 2001). Finally, CTRW was also used for breakthrough curve analysis of numerical experiments mimicking transport in fault zones (O'Brien et al, 2003b,a).

4.4 Other applications

As explained in section 2.4, CTRW has been largely used as average transport model; in fact the ensemble particle motions in many quenched disordered systems obey a CTRW dynamic (Berkowitz et al, 2006). For this reason and motivated by the results of single particle tracking for diffusion in heterogeneous media, CTRW models has been used to study the question of ergodicity in complex media (Bel and Barkai, 2005; He et al, 2008; Barkai et al, 2012; Metzler et al, 2014). More recently, Dentz et al (2016) used TDRW to study the self-averaging properties and ergodicity of subdiffusion in random media. As seen in section 2.3, TDRW is equivalent to the discretized ADE and allows to distinguish between ensemble particle motion (CTRW) and diffusive random motion in a single realization.

Todays, the limits of RW and TDRW methods are for some extent in the reconstruction of concentration fields and their use for reactive transport simulations involving non-linear chemical reactions. A few methods have been developed to reconstruct the concentration field a posteriori from the random walkers while keeping their independence [Fernandez-Garcia and Sanchez-Vila, 2011]. Others decouple the advective and dispersive terms, simulate the advective term with a particle tracking method and the dispersive term with Smoothed Particle Hydrodynamic (SPH) methods (Herrera et al, 2009, 2010; Herrera and Beckie, 2013). With SPH, each particle is considered as an elementary volume of water containing solutes and exchanging mass with the neighboring volumes according to a prescribed interpolation kernel, which is also eventually used to reconstruct the concentration field. With this method, random walkers remain independent and dispersive processes stem from the particle positions without feedback from the concentration field to the particle displacements. Heterogeneous distributions of particles with rarefaction in low flow zones may critically decrease the accuracy of calculated concentrations. Increasing the particle number or performing particle re-meshing are sometimes necessary and impact numerical performances or numerical diffusion. To summarize, these methods are intermediary between RW, full SPH, and Particle Strength Exchange (PSE) methods that introduce the influence of concentration fields on the motion of particles and subsequent interdependence of the particles (Beaudoin et al, 2002, 2003; Monaghan, 2005; Tartakovsky and Meakin, 2006). Like SPH and PSE, several implementations of RW and TDRW can be considered as mesh-free methods that can easily adapt their resolution to local physical or chemical properties without extensive re-meshing efforts. When chemistry mostly consists of fluid-rock interactions rather of reactions in solution, particles can again be taken as water volumes or "finite cells" with their embedded solutes chemically interacting with the solid (Besnard et al, 2011; Sun, 1999, 2002). This role is especially well suited when dispersion is dominated by fluid-rock interactions or mobile-immobile types of exchanges (Cirpka, 2005; Michalak

and Kitanidis, 2000). More generally, appropriate combination of these Lagrange-based methods could be welcomed to locally separate solute dispersion from solute mixing. Dispersion would be simulated as particle movements, and mixing as exchanges between particles. The sharing between dispersion and mixing could be derived from some local properties of the particle position or of the reconstructed concentration pattern (de Dreuzy et al, 2012; Le Borgne et al, 2011, 2015). In this framework, RW and TDRW methods have a strong capacity to integrate detailed physical processes beyond the resolution of the coarse mesh-cell scale that may be used in practical applications, for example by means of the flexibility offered by the choice of the transition time distribution.

Finally, RW methods have been used at the small scale to model heat transfer (Emmanuel and Berkowitz, 2007) and emulsion transport in porous media (Cortis and Ghezzehei, 2007). At a larger scale, additional applications are related to the interpretation of hydraulic pumping tests in heterogeneous porous media (Cortis and Knudby, 2006), to the impact of matrix heterogeneity on the residence times of solutes in fractured media (Robinet et al, 2007), and to the interpretation of water age data sampled under pumping conditions (Leray et al, 2014).

5 Conclusions

RW methods have become a mature tool with skills to handle efficiently diffusion processes or advection dispersion in porous media riddled with multiscale quenched heterogeneities, including complex fracture patterns. The spatial scales of interest range from nanometers (molecules) and microns for simulations over images of the pore space to kilometers for field scale investigations. Radially convergent flows can also be accounted for. The RW class of methods is usually easy to implement and possesses a natural structure adapted to High Performance Computing (HPC), which in turn renders the methods powerful and suited to up-scaling applications. CTRW and TDRW have earned a rigorous probabilistic connection with finite volume methods which allow us to compare the calculations with the conventional equations of the physics of flow and transport. All these features provide a natural framework for elaborating new theories of normal or anomalous large-scale dispersion as they give a natural picture of solute mixing and spreading. RW techniques highlight the competition between advection, dispersion and the underlying quenched disorder of the medium. The effects of retention and of chemical reactions can also be modeled.

Future research might take several directions. To mention a few, it could be worth finding some robust parameterizations of the scattering kernels $M(\mathbf{a}, t; \mathbf{x}-\mathbf{a})$ or of the transfer functions $f(.)$ and link them with the medium disorder (Noetinger and Gautier, 1998; Liu et al, 2000). Adsorption processes and chemical reactions could also be simulated, at least in the linear regime, by adding a suitable variable characterizing the state of the particle during its random motion. For example, one could consider a two state vector denoted $\mathbf{x}(t) \rightarrow \mathbf{x}(t) \begin{bmatrix} c_1(t) \\ c_2(t) \end{bmatrix}$, in which the indicator of the state of the particle $c_1(t)$ can take the value 0 or 1, $(c_2(t) = 1 - c_1(t))$. These binary states could correspond to the fact that a particle is in the fractures or not, or is in the phase of a specific chemical component, etc... Choosing suitable transition probabilities for the elementary time step in the corresponding Langevin

formulation (thus allowing the particle to swap between states randomly) would provide a direct RW interpretation of the double porosity equations (60) or of chemical reactions in solution and with the solid. Another important topic is being able to generalize RW methods with the aim of coupling explicitly the particle concentrations and properties of fluid and fluid flow, leading for instance to viscous or density driven fingering patterns. The difficulty resides in the fact that at any time flow depends on the whole map of particle concentrations with the consequence of manipulating fully coupled flow-transport problem (Saffman and Taylor, 1958; Dagan, 1989) where RW methods lose efficiency (cumbersome calculations of local concentrations, breaks in parallel chains of computations, limitations for solving non-linearity, etc.) At first glance, the framework of independent particles undergoing RW seems not suited to that kind of complex coupling with non-linear relationships between flow and transport. Nevertheless, the successful RW picture of Diffusion Limited Aggregation (DLA) provided in Witten and Sander (1983) and Tang (1985) and corresponding to fluid fingering with infinite mobility contrasts gives hope that RW could come out as a relevant method to address that kind of issues. In particular, framing the macroscopic depiction of the motion of unstable interfaces in random quenched disordered media could be undertaken by relying upon a RW approach with particle motion conditioned by the degrees of freedom describing the fluid fronts (Nœtinger et al, 2004; Tallakstad et al, 2009; Teodorovich et al, 2011).

In addition, we can mention a last application of RW to calibrate the large-scale model parameters that are needed in the traded or industrial simulators built for the purpose of diverse applications at the field scale. Among these practical tools, some operational methods use RW techniques in order to sample the admissible space of the parameters to be calibrated. Such approaches were followed by (Hu, 2000; Romary, 2009). Increasingbly popular Kalman Filtering approaches (Oliver et al, 1997; Evensen, 2009; Aanonsen et al, 2009) may also be included as being a particular class of RW methods applied at the reservoir scale.

Finally, this review tentatively showed that the RW methods and more generally the Lagrangian approaches to fluid dynamics, was still a fairway for fertile research activity in the domain of flow and transport in porous (fractured) media. Comparisons with other methods were not considered to emphasize the general elegance of random walk methods in the way they tackle various problems.

A Langevin equation and Fokker Planck equation

In this section, we show the equivalence between the Fokker-Planck equation (1) and the Langevin equation (2). To this end, we use a duality argument. Let $f(\mathbf{x})$ be a twice differentiable function. We consider now the average $\langle f[\mathbf{x}(t)]\rangle$. By virtue of (3), this average may be written as

$$\langle f[\mathbf{x}(t)]\rangle = \int d\mathbf{x} P(\mathbf{x},t) f(\mathbf{x}). \tag{57}$$

We consider now $\langle f[\mathbf{x}(t+dt)]\rangle$. To this end, we note that $\mathbf{x}(t+dt)$ is according to (2)

$$\mathbf{x}(t+dt) = \mathbf{x}(t) + \mathbf{v}[\mathbf{x}(t)]dt + \sqrt{2\mathbf{B}[\mathbf{x}(t)]}\cdot\eta(t) \equiv \mathbf{x}(t) + \Delta\mathbf{x}(t) \tag{58}$$

where we use the Ito interpretation of the stochastic integral (Risken, 1996); $\boldsymbol{\eta}(t)$ is a Gaussian random variable with 0 mean and unit variance. Taylor expansion of $f[\mathbf{x}(t)+\Delta\mathbf{x}(t)]$ consistently up to order dt then gives

$$f[\mathbf{x}(t+dt)] - f[\mathbf{x}(t)] = \nabla f[\mathbf{x}(t)]\cdot\mathbf{v}[\mathbf{x}(t)]dt + \nabla\otimes\nabla f[\mathbf{x}(t)] : \mathbf{B}[\mathbf{x}(t)]dt. \tag{59}$$

It is worthwile noting that this equation is also called the Ito formula, or chain rule of stochastic calculus (Risken, 1996). Taking the average of (59) and using (57) gives after integration by parts the Fokker-Planck equation (1).

B Dual-porosity models

Fractured porous media are characterized by a high property contrast between fractures and matrix. This leads to introducing a new class of models, starting from the steady state double porosity models (Barenblatt and Zheltov, 1960; Warren and Root, 1963) as derived by Arbogast et al (1990) and Quintard and Whitaker (1993) that couple matrix and fracture by means of a linear exchange term:

$$\begin{cases} \phi_f V_f \frac{\partial P_f(\mathbf{x},t)}{\partial t} = D_f \nabla^2 P_f(\mathbf{x},t) + Q(\mathbf{x},t) \\ \phi_m V_m \frac{\partial P_m(\mathbf{x},t)}{\partial t} = D_m \nabla^2 P_m(\mathbf{x},t) - Q(\mathbf{x},t). \end{cases} \tag{60}$$

Here, $\phi_f V_f$ and $\phi_m V_m$ represent respectively the overall proportions of fracture and matrix volumes (weighted by the relevant porosity and compressibility). The operation $*$ represents a convolution operator. The model is closed once the interporosity flux $Q(\mathbf{x},t)$ is expressed as a function of $P_f(\mathbf{x},t)$ and $P_m(\mathbf{x},t)$. In the steady state case, $Q(\mathbf{x},t)$ is given by:

$$Q(\mathbf{x},t) = \lambda \left(P_m(\mathbf{x},t) - P_f(\mathbf{x},t) \right). \tag{61}$$

The transfer coefficient λ, reciprocal of a time depends mainly on the geometry of the matrix blocks. It is proportional to D_m. Its determination from the detailed DFN geometry will be discussed in section 3.4.1.

More general models using memory functions accounting for more details of the diffusion inside the matrix can be introduced (Odeh, 1965; de Swaan, 1976; Carslaw and Jaeger, 1986; Daviau, 1986; Chen, 1989; de Swann and Ramirez-Villa, 1993). These models belongs to the general class of Multiple Rate Mass Transfer (MRMT) models or Multiple Interacting Continua (MINC) (Narasimhan and Pruess, 1988; Haggerty and Gorelick, 1995; de Dreuzy et al, 2013). These models correspond to quite different formulations of the same physics differ through the formulation of the exchange term. The latter appears as a time convolution expressed by:

$$Q(\mathbf{x},t) = \int_0^t G(t-\tau) \left(\frac{d(P_m(\mathbf{x},\tau) - P_f(\mathbf{x},\tau))}{d\tau} \right) d\tau. \tag{62}$$

In all cases, the exchange kernel $G(t)$ is scaled by a parameter λ which depends only on the geometry of the matrix blocks. It was shown in Landereau et al (2001) and Babey et al (2015) that Multiple porosity models, MRMT models and transient models are equivalent and correspond to different formulations of the same idea.

In most cases, the term $D_m \nabla^2 P_m(\mathbf{x},t)$ may be neglected in the double porosity equations (60), so $P_m(\mathbf{x},t)$ may be eliminated from the equations to provide the following generic form:

$$\int_0^t d\tau (\phi_f V_f \delta(t-\tau) + \phi_m V_m f(t-\tau)) \frac{\partial P_f(\mathbf{x},\tau)}{\partial \tau} = \nabla.(D_f \nabla P_f(\mathbf{x},t)). \tag{63}$$

The quantity $f(t)$ is the time dependent exchange function. Introducing the average pressure in the fractures $< \hat{P}_f > (t)$ solution of the following initial value problem:

$$\phi(\mathbf{x}) \frac{\partial P_f(\mathbf{x},t)}{\partial t} = \nabla.(D(\mathbf{x}) \nabla P_f(\mathbf{x},t)) \tag{64}$$

$$\forall \mathbf{x} \in \Omega_f \, P_f(\mathbf{x}, t=0) = 1 \tag{65}$$

$$\forall \mathbf{x} \in \Omega_m \, P_f(\mathbf{x}, t=0) = 0 \tag{66}$$

$$< P_f > (t) = \frac{1}{|\Omega_f|} \int_{\Omega_f} d\mathbf{x} P_f(\mathbf{x},t) \tag{67}$$

It is possible to show the following relation in the Laplace domain:

$$< P_f > (s) = \frac{\phi_f V_f}{s(\phi_f V_f + \phi_m V_m f(s))}. \tag{68}$$

The practical interest of introducing the $f(s)$ function is that it can be shown that the general solution of a double porosity system (60) can be directly related to a solution of a single porosity equation replacing the argument s of the single porosity solution by the argument $s(\phi_f V_f + s\phi_m V_m f(s))$. The large amount of analytical single porosity solutions that are well known is sufficient for most practical situations. This means that all the double porosity behavior is captured by $f(s)$, which appears to be a renormalized apparent storativity. The initial value problem (67) defining $< \hat{P}_f > (t)$ has in turn a simple RW interpretation. The quantity $< P_f > (t)$ corresponds to the average proportion of particle undergoing RW (with diffusivity D_m) that belongs to the fractures at time t given they was released at a random location in the fractures at time $t = 0$. In the steady state case, the function $f(s)$ is given by (Noetinger and Estebenet, 2000; Noetinger et al, 2001a):

$$f(s) = \frac{\lambda}{\phi_m V_m s + \lambda}. \tag{69}$$

It appears that λ is a characteristic diffusion time in the matrix. Explicit expressions may be given for $f(s)$ for either a layered medium, or for spherical blocks:

- for the layered case

$$f(s) = \sqrt{\frac{\lambda}{3sV_m}} \tanh \sqrt{\frac{3V_m s}{\lambda}}, \tag{70}$$

- for the spherical case

$$f(s) = \frac{\lambda}{5sV_m} \left(\sqrt{\frac{15V_m s}{\lambda}} \mathrm{cotanh} \sqrt{\frac{15\mathrm{V_m s}}{\lambda}} - 1 \right). \tag{71}$$

These generic forms, or others can be used for large scale applications, solving (63) using any numerical approach. It remains to be able to evaluate the transfer coefficient λ or the full $f(t)$ function. This is the objective of section 3.4.1.

References

Aanonsen SI, Nævdal G, Oliver DS, Reynolds AC, Vallès B, et al (2009) The ensemble kalman filter in reservoir engineering–a review. Spe Journal 14(03):393–412

Abramowitz M, Stegun IA (1972) Handbook of Mathematical Functions. Dover Publications, New York

Acuna JA, Yortsos YC (1995) Application of fractal geometry to the study of networks of fractures and their pressure transient. Water Resources Research 31(3):527–540, DOI 10.1029/94WR02260

de Anna P, Le Borgne T, Dentz M, Tartakovsky A, Bolster D, Davy P (2013) Flow intermittency, dispersion, and correlated continuous time random walks in porous media. Physical Review Letters 110(18), DOI 10.1103/PhysRevLett.110.184502

Arbogast T, Douglas J, Hornung U (1990) Derivation of the double porosity model of single phase flow via homogeneization theory. SIAM J Math Anal 21(4):823–836

de Arcangelis L, Koplik J, Redner S, Wilkinson D (1986) Hydrodynamic dispersion in network models of porous media. Physical Review Letters 57(8):986–999, DOI 10.1103/PhysRevLett.57.996

Aris R (1956) On the dispersion of a solute in a fluid flowing through a tube. In: Proceedings of the Royal Society of London A-Mathematical and Physical Sciences, vol 235, pp 67–77, DOI 10.1098/rspa.1956.0065

Babey T, de Dreuzy J-R, Casenave C (2015) Multi-Rate Mass Transfer (MRMT) models for general diffusive porosity structures. Advances in Water Resources 76:146–156, DOI 10.1016/j.advwatres.2014.12.006

Barenblatt GI, Zheltov YP (1960) Fundamental equations of homogeneous liquids in fissured rocks. Dokl Akad Nauk SSSR 132(3):545–548

Barkai E, Garini Y, Metzler R (2012) Strange kinetics of single molecules in living cells. Physics Today 65(8):29–35, DOI 10.1063/PT.3.1677

Barker JA (1988) A generalized radial flow model for hydraulic tests in fractured rock. Water Resources Research 24(10):1796–1804, DOI 10.1029/WR024i010p01796
Barthelemy P, Bertolotti J, Wiersma DS (2008) A Lévy flight for light. Nature 453(7194):495–498, DOI 10.1038/nature06948
Bear J (1973) Dynamics of Fluids in Porous Media. Dover Publications
Beaudoin A, de Dreuzy JR (2013) Numerical assessment of 3-D macrodispersion in heterogeneous porous media. Water Resources Research 49(5):2489–2496, DOI 10.1002/wrcr.20206
Beaudoin A, Huberson S, Rivoalen E (2002) Anisotropic particle method. Comptes Rendus Mecanique 330(1):51–56, DOI 10.1016/S1631-0721(02)01429-8
Beaudoin A, Huberson S, Rivoalen E (2003) Simulation of anisotropic diffusion by means of a diffusion velocity method. Journal of Computational Physics 186(1):122–135, DOI 10.1016/S0021-991(03)00024-X
Beaudoin A, de Dreuzy JR, Erhel J (2007) An efficient parallel tracker for advection-diffusion simulations in heterogeneous porous media. In: Springer-Verlag B, Heidelberg (eds) Europar, pp 28–31
Beaudoin A, de Dreuzy JR, Erhel J (2010) Numerical Monte Carlo analysis of the influence of pore-scale dispersion on macrodispersion in 2-D heterogeneous porous media. Water Resources Research 46:12, DOI 10.1029/2010WR009576
Bechtold M, Vanderborght J, Ippisch O, Vereecken H (2011) Efficient random walk particle tracking algorithm for advective-dispersive transport in media with discontinuous dispersion coefficients and water contents. Water Resources Research 47:10, DOI 10.1029/2010WR010267
Becker MW, Shapiro AM (2003) Interpreting tracer breakthrough tailing from different forced-gradient tracer experiment configurations in fractured bedrock. Water Resources Research 39(1):1024, DOI 10.1029/2001WR001190
Bel G, Barkai E (2005) Weak ergodicity breaking in the continuous-time random walk. Physical Review Letters 94:240,602, DOI 10.1103/PhysRevLett.94.240602
Berkowitz B, Balberg I (1993) Percolation theory and its application to groundwater hydrology. Water Resources Research 29(4):775–794, DOI 10.1029/92WR02707
Berkowitz B, Scher H (1997) Anomalous transport in random fracture networks. Physical Review Letters 79(20):4038–4041, DOI 10.1103/PhysRevLett.79.4038
Berkowitz B, Scher H (1998) Theory of anomalous chemical transport in random fracture networks. Physical Review E 57(5):5858–5869, DOI 10.1103/PhysRevE.57.5858
Berkowitz B, Naumann C, Smith L (1994) Mass-transfer at fracture intersections - An evaluation of mixing models. Water Resources Research 30(6):1765–1773, DOI 10.1029/94WR00432
Berkowitz B, Scher H, Silliman S (2000) Anomalous transport in laboratory-scale, heterogeneous porous media. Water Resources Research 36(1):149–158, DOI 10.1029/1999WR900295
Berkowitz B, Klafter J, Metzler R, Scher H (2002) Physical pictures of transport in heterogeneous media: Advection-dispersion, random-walk, and fractional derivative formulations. Water Resources Research 38(10):1191, DOI 10.1029/2001WR001030
Berkowitz B, Cortis A, Dentz M, Scher H (2006) Modeling non-Fickian transport in geological formations as a continuous time random walk. Reviews of Geophysics 44(2):RG2003, DOI 10.1029/2005RG000178
Besnard K, de Dreuzy JR, Davy P, Aquilina L (2011) A modified lagrangian-volumes method to simulate nonlinearly and kinetically sorbing solute transport in heterogeneous porous media. Journal of Contaminant Hydrology 120-21(SI):89–98, DOI 10.1016/j.jconhyd.2010.03.004
Bijeljic B, Mostaghimi P, Blunt M (2013a) Insights into non-fickian solute transport in carbonates. Water Resources Research 49(5):2714–2728
Bijeljic B, Raeini A, Mostaghimi P, Blunt M (2013b) Predictions of non-fickian solute transport in different classes of porous media using direct simulation on pore-scale images. Physical Review E 87(1), DOI 10.1103/PhysRevE.87.013011
Boano F, Packman AI, Cortis A, Revelli R, Ridolfi L (2007) A continuous time random walk approach to the stream transport of solutes. Water Resources Research 43(10), DOI 10.1029/2007WR006062
Bodin J (2015) From analytical solutions of solute transport equations to multidimensional time-domain random walk (TDRW) algorithms. Water Resources Research 51(3):1860–1871, DOI 10.1002/2014WR015910
Bodin J, Porel G, Delay F (2003) Simulation of solute transport in discrete fracture networks using the time domain random walk method. Earth and Planetary Science Letters 208(3-

4):297–304, DOI 10.1016/S0012-821X(03)00052-9
Bodin J, Porel G, Delay F, Ubertosi F, Bernard S, de Dreuzy JR (2007) Simulation and analysis of solute transport in 2D fracture/pipe networks: The SOLFRAC program. Journal of Contaminant Hydrology 89(1-2):1–28, DOI 10.1016/j.jconhyd.2006.07.005
Bouchaud JP, Georges A (1990) Anomalous diffusion in disordered media: statistical mechanisms, models and physical applications. Physics Reports 195(4-5):127–293, DOI 10.1016/0370-1573(90)90099-N
Brezzi F, Fortin M (1991) Mixed and Hybrid Finite Element Methods. Springer, Berlin
Bromly M, Hinz C (2004) Non-fickian transport in homogeneous unsaturated repacked sand. Water Resources Research 40(7), DOI 10.1029/2003WR002579
Bruderer C, Bernabé Y (2001) Network modeling of dispersion: transition from taylor dispersion in homogeneous networks to mechanical dispersion in very heterogeneous ones. Water Resources Research 37(4):897–908, DOI 10.1029/2000WR900362
Cacas MC, Ledoux E, de Marsily G, Barbreau A, Calmels P, Gaillard B, Margritta R (1990) Modeling fracture flow with a stochastic discrete network: Calibration and validation. 2. The transport model. Water Resources Research 26(3):491–500, DOI 10.1029/WR026i003p00491
Carrera J, Sanchez-Vila X, Benet I, Medina A, Galarza G, Guimera J (1998) On matrix diffusion: formulations, solution methods and qualitative effects. Hydrogeology Journal 6(1):178–190, DOI 10.1007/s100400050143
Carslaw HS, Jaeger JC (1986) Conduction of heat in solids. Oxford science publications, Clarendon Press
Chang J, Yortsos YC (1990) Pressure transient analysis of fractal reservoirs. SPE Formation Evaluation 5(1), DOI 10.2118/18170-PA
Charlaix E, Guyon E, Roux S (1987) Permeability of a random array of fractures of widely varying apertures. Transport in Porous Media 2(1):31–43
Chavent G, Roberts JE (1991) A unified physical presentation of mixed, mixed-hybrid finite elements and standard finite difference approximations for the determination of velocities in waterflow problems. Advances in Water Resources 14(6):329–348, DOI 10.1016/0309-1708(91)90020-O
Chen ZX (1989) Transient Flow of Slightly Compressible Fluids Through Double-porosity, Double-permeability systems - A state-of-the-art review. Transport in Porous Media 4(2):147–184, DOI 10.1007/BF00134995
Cirpka OA (2005) Effects of sorption on transverse mixing in transient flows. Journal of Contaminant Hydrology 78(3):207–229, DOI 10.1016/j.jconhyd.2005.05.008
Cordes C, Kinzelbach W (1992) Continuous groundwater velocity field and path lines in linear, bilinear and trilinear finite elements. Water Resources Research 28(11):2903–2911, DOI 10.1029/92WR01686
Cordes C, Kinzelbach W (1996) Comment on "Application of the mixed hybrid finite element approximation in a groundwater flow model: Luxury or necessity?". Water Resources Research 32(6):1905–1911, DOI 10.1029/96WR00567
Cortis A, Berkowitz B (2004) Anomalous transport in "classical " soil and sand columns. Soil Science Society of America Journal 68(5):1539–1548
Cortis A, Ghezzehei TA (2007) On the transport of emulsions in porous media. Journal of Colloid and Interface Science 313(1):1–4, DOI 10.1016/j.jcis.2007.04.021
Cortis A, Knudby C (2006) A continuous time random walk approach to transient flow in heterogeneous porous media. Water Resources Research 42(10), DOI 10.1029/2006WR005227
Cvetkovic V, Frampton A (2012) Solute transport and retention in three-dimensional fracture networks. Water Resources Research 48, DOI 10.1029/2011WR011086
Cvetkovic V, Painter S, Outters N, Selroos JO (2004) Stochastic simulation of radionuclide migration in discretely fractured rock near the Äspö Hard Rock Laboratory. Water Resources Research 40(2), DOI 10.1029/2003WR002655
Dagan G (1989) Flow and transport in porous formations. Springer-Verlag GmbH & Co. KG.
Danckwerts PV (1952) The definition and measurements of some characteristics of mixtures. Appl Sci Res 3(4):279–296
Daviau F (1986) Interprétation des essais de puits, les méthodes nouvelles, technip edn. Publications de l'institut francais du pétrole, Paris
Delay F, Bodin J (2001) Time domain random walk method to simulate transport by advection-dispersion and matrix diffusion in fractured networks. Geophysical Research Letters 28(21):4051–4054, DOI 10.1029/2001GL013698

Delay F, Porel G, Sardini P (2002) Modelling diffusion in a heterogeneous rock matrix with a time-domain lagrangian method and an inversion procedure. Comptes Rendus Geoscience 334(13):967–973, DOI 10.1016/S1631-0713(02)01835-7

Delay F, Ackerer P, Danquigny C (2005) Simulating solute transport in porous or fractured formations using random walk particle tracking: A review. Vadose Zone Journal 4(2):360–379, DOI 10.2136/vzj2004.0125

Delorme M, Daniel JM, Kada-Kloucha C, Khvoenkova N, Schueller S, Souque C (2013a) An efficient model to simulate reservoir stimulation and induced microseismic events on 3D discrete fracture network for unconventional reservoirs. Unconventional Resources Technology Conference, 12-14 August, Denver, Colorado, USA, pp 1433–1442, DOI 10.1190/URTEC2013-146

Delorme M, Mota RO, Khvoenkova N, Fourno A, Noetinger B (2013b) A methodology to characterize fractured reservoirs constrained by statistical geological analysis and production: a real field case study. Geological Society, London, Special Publications 374(1):273–288

Dentz M, Cortis A, Scher H, Berkowitz B (2004) Time behavior of solute transport in heterogeneous media: transition from anomalous to normal transport. Advances in Water Resources 27(2):155–173, DOI 10.1016/j.advwatres.2003.11.002

Dentz M, Le Borgne T, Englert A, Bijeljic B (2011) Mixing, spreading and reaction in heterogeneous media: A brief review. Journal of Contaminant Hydrology 120-21(SI):1–17, DOI 10.1016/j.jconhyd.2010.05.002

Dentz M, Gouze P, Russian A, Dweik J, Delay F (2012) Diffusion and trapping in heterogeneous media: An inhomogeneous continuous time random walk approach. Advances in Water Resources 49:13–22, DOI 10.1016/j.advwatres.2012.07.015

Dentz M, Russian A, Gouze P (2016) Self-averaging and ergodicity of subdiffusion in quenched random media. Physical Review E in press

Dershowitz W, Miller I (1995) Dual porosity fracture flow and transport. Geophysical Research Letters 22(11):1441–1444, DOI 10.1029/95GL01099

de Dreuzy JR, Davy P, Berkowitz B (2001) Advective transport in the percolation backbone in two dimensions. Physical Review E 64(5)

de Dreuzy JR, Beaudoin A, Erhel J (2007) Asymptotic dispersion in 2D heterogeneous porous media determined by parallel numerical simulations. Water Resources Research 43(10), DOI 10.1029/2006WR005394

de Dreuzy JR, Carrera J, Dentz M, Le Borgne T (2012) Time evolution of mixing in heterogeneous porous media. Water Resources Research 48, DOI 10.1029/2011WR011360

de Dreuzy JR, Rapaport A, Babey T, Harmand J (2013) Influence of porosity structures on mixing-induced reactivity at chemical equilibrium in mobile/immobile Multi-Rate Mass Transfer (MRMT) and Multiple INteracting Continua (MINC) models. Water Resources Research 49(12):8511–8530, DOI 10.1002/2013WR013808

Edery Y, Guadagnini A, Scher H, Berkowitz B (2014) Origins of anomalous transport in heterogeneous media: Structural and dynamic controls. Water Resources Research 50(2):1490–1505, DOI 10.1002/2013WR015111

Einstein A (1956) Investigations on the theory of the Brownian movement. Dover Publication, New York

Emmanuel S, Berkowitz B (2007) Continuous time random walks and heat transfer in porous media. Transport in Porous Media 67(3):413–430, DOI 10.1007/s11242-006-9033-z

Evensen G (2009) Data assimilation: the ensemble Kalman filter. Springer Science & Business Media

Fleury M, Bauer D, Néel M (2015) Modeling of super-dispersion in unsaturated porous media using nmr propagators. Microporous and Mesoporous Materials 205:75–78

Geiger S, Cortis A, Birkholzer J (2010) Upscaling solute transport in naturally fractured porous media with the continuous time random walk method. Water Resources Research 46(12)

Gjetvaj F, Russian A, Gouze P, Dentz M (2015) Dual control of flow field heterogeneity and immobile porosity on non-Fickian transport in Berea sandstone. Water Resources Research 51(10):8273–8293, DOI 10.1002/2015WR017645

Gouze P, Luquot L (2011) X-ray microtomography characterization of porosity, permeability and reactive surface changes during dissolution. Journal of Contaminant Hydrology 120-121(SI):45–55, DOI 10.1016/j.jconhyd.2010.07.004

Gouze P, Le Borgne T, Leprovost R, Lods G, Poidras T, Pezard P (2008a) Non-Fickian dispersion in porous media: 1. Multiscale measurements using single-well injection withdrawal tracer tests. Water Resources Research 44(6), DOI 10.1029/2007WR006278

Gouze P, Melean Y, Le Borgne T, Dentz M, Carrera J (2008b) Non-fickian dispersion in porous media explained by heterogeneous microscale matrix diffusion. Water Resources Research 44(11), DOI 10.1029/2007WR006690

Guillon V, Fleury M, Bauer D, Néel MC (2013) Superdispersion in homogeneous unsaturated porous media using NMR propagators. Physical Review E 87(4), DOI 10.1103/PhysRevE.87.043007

Guillon V, Bauer D, Fleury M, Néel MC (2014) Computing the longtime behaviour of NMR propagators in porous media using a pore network random walk model. Transport in Porous Media 101(2):251–267, DOI 10.1007/s11242-013-0243-x

Haggerty R, Gorelick SM (1995) Multiple-rate mass transfer for modeling diffusion and surface reactions in media with pore-scale heterogeneity. Water Resources Research 31(10):2383–2400, DOI 10.1029/95WR01583

Haggerty R, McKenna SA, Meigs LC (2000) On the late time behavior of tracer test breakthrough curves. Water Resources Research 36(12):3467–3479, DOI 10.1029/2000WR900214

Hatano Y, Hatano N (1998) Dispersive transport of ions in column experiments: An explanation of long-tailed profiles. Water Resources Research 34(5):1027–1033, DOI 10.1029/98WR00214

He Y, Burov S, Metzler R, Barkai E (2008) Random time-scale invariant diffusion and transport coefficients. Physical Review Letters 101(5), DOI 10.1103/PhysRevLett.101.058101

Herrera PA, Beckie RD (2013) An assessment of particle methods for approximating anisotropic dispersion. International Journal for Numerical Methods in Fluids 71(5):634–651, DOI 10.1002/fld.3676

Herrera PA, Massabo M, Beckie RD (2009) A meshless method to simulate solute transport in heterogeneous porous media. Advances in Water Resources 32(3):413–429, DOI 10.1016/j.advwatres.2008.12.005

Herrera PA, Valocchi AJ, Beckie RD (2010) A multidimensional streamline-based method to simulate reactive solute transport in heterogeneous porous media. Advances in Water Resources 33(7):711–727, DOI 10.1016/j.advwatres.2010.03.001

Holzner M, Morales VL, Willmann M, Dentz M (2015) Intermittent lagrangian velocities and accelerations in three-dimensional porous medium flow. Physical Review E 92(1), DOI 10.1103/PhysRevE.92.013015

Hoteit H, Erhel J, Mos R, Philippe B, Ackerer P (2002a) Numerical reliability for mixed methods applied to flow problems in porous media. Computational Geosciences 6(2):161–194, DOI 10.1023/A:1019988901420

Hoteit H, Mose R, Younes A, Lehmann F, Ackerer P (2002b) Three-dimensional modeling of mass transfer in porous media using the mixed hybrid finite elements and the random-walk methods. Mathematical Geology 34(4):435–456, DOI 10.1023/A:1015083111971

Hu LY (2000) Gradual deformation and iterative calibration of gaussian-related stochastic models. Mathematical Geology 32(1):87–108

Jimenez-Hornero F, Giraldez J, Laguna A, Pachepsky Y (2005) Continuous time random walks for analyzing the transport of a passive tracer in a single fissure. Water Resources Research 41(4), DOI 10.1029/2004WR003852

Kang PK, Dentz M, Le Borgne T, Juanes R (2011) Spatial Markov model of anomalous transport through random lattice networks. Physical Review Letters 107(18), DOI 10.1103/PhysRevLett.107.180602

Kang PK, de Anna P, Nunes JP, Bijeljic B, Blunt M, Juanes R (2014) Pore-scale intermittent velocity structure underpinning anomalous transport through 3D porous media. Geophysical Research Letters 41(17):6184–6190, DOI 10.1002/2014GL061475

Kang PK, Le Borgne T, Dentz T, Bour O, Juanes R (2015) Impact of velocity correlation and distribution on transport in fractured media: field evidence and theoretical model. Water Resources Research 51(2):940–959, DOI 10.1002/2014WR015799

Kenkre VM, Montroll EW, Shlesinger MF (1973) Generalized master equations for continuous-time random walks. J Stat Phys 9(1):45–50

Khvoenkova N, Delorme M (2011) An optimal method to model transient flows in 3D discrete fracture network. IAMG conference 2011:1238–1249, DOI 10.5242/iamg.2011.0088

Kim IC, Torquato S (1992) Effective conductivity of suspensions of overlapping spheres. Journal of Applied Physics 71(6):2727–2735, DOI 10.1063/1.351046

Kinzelbach W (1988) The random walk method in pollutant transport simulation. In: Groundwater flow and quality modelling, Springer, pp 227–245

Kinzelbach W, Uffink G (1991) The random walk method and extensions in groundwater modelling, vol Transport Processes in Porous Media. Springer, Netherlands
Kitanidis P (1994) The concept of the dilution index. Water Resources Research 30(7):2011–2026, DOI 10.1029/94WR00762
Klafter J, Silbey R (1980) Derivation of the continuous-time random-walk equation. Physical Review Letters 44(2):55–58, DOI 10.1103/PhysRevLett.44.55
Klafter J, Sokolov I (2005) Anomalous diffusion spreads its wings. Phys World 18(8):29–32
Koplik J, Redner S, Wilkinson D (1988) Transport and dispersion in random networks with percolation disorder. Physical Review A 37(7):2619–2636, DOI 10.1103/PhysRevA.37.2619
Kosakowski G (2004) Anomalous transport of colloids and solutes in a shear zone. Journal of Contaminant Hydrology 72(1-4):23–46, DOI 10.1016/j.jconhyd.2003.10.005
Kosakowski G, Berkowitz B (1999) Flow pattern variability in natural fracture intersections. Geophysical Research Letters 26(12):1765–1768, DOI 10.1029/1999GL900344
Kosakowski G, Berkowitz B, Scher H (2001) Analysis of field observations of tracer transport in a fractured till. Journal of Contaminant Hydrology 47(1):29–51, DOI 10.1016/S0169-7722(00)00140-6
LaBolle EM, Quastel J, Fogg GE (1998) Diffusion theory for transport in porous media: Transition-probability densities of diffusion processes corresponding to advection-dispersion equations. Water Resources Research 34(7):1685–1693
Landereau P, Noetinger B, Quintard M (2001) Quasi-steady two-equation models for diffusive transport in fractured porous media: large-scale properties for densely fractured systems. Advances in Water Resources 24(8):863–876, DOI 10.1016/S0309-1708(01)00015-X
Le Borgne T, Gouze P (2008) Non-fickian dispersion in porous media: 2. Model validation from measurements at different scales. Water Resources Research 44(6), DOI 10.1029/2007WR006279
Le Borgne T, Dentz M, Carrera J (2008a) A Lagrangian statistical model for transport in highly heterogeneous velocity fields. Physical Review Letters 101(9), DOI 10.1103/PhysRevLett.101.090601
Le Borgne T, Dentz M, Carrera J (2008b) Spatial Markov processes for modeling lagrangian particle dynamics in heterogeneous porous media. Physical Review E 78(2,2), DOI 10.1103/PhysRevE.78.026308
Le Borgne T, Dentz M, Bolster D, Carrera J, de Dreuzy JR, Davy P (2010) Non-fickian mixing: Temporal evolution of the scalar dissipation rate in heterogeneous porous media. Advances in Water Resources 33(12):1468–1475, DOI 10.1016/j.advwatres.2010.08.006
Le Borgne T, Dentz M, Davy P, Bolster D, Carrera J, de Dreuzy JR, Bour O (2011) Persistence of incomplete mixing: A key to anomalous transport. Physical Review E 84(1,2), DOI 10.1103/PhysRevE.84.015301
Le Borgne T, Dentz M, Villermaux E (2013) Stretching, coalescence and mixing in porous media. Physical Review Letters 110(20), DOI 10.1103/PhysRevLett.110.204501
Le Borgne T, Dentz M, Villermaux E (2015) The lamellar description of mixing in porous media. Journal of Fluid Mechanics 770:458–498, DOI 10.1017/jfm.2015.117
Lejay A, Pichot G (????) Simulating diffusion processes in discontinuous media: Benchmark tests. Journal of Computational Physics
Leray S, de Dreuzy JR, Aquilina L, Vergnaud-Ayraud V, Labasque T, Bour O, Le Borgne T (2014) Temporal evolution of age data under transient pumping conditions. Journal of Hydrology 511:555–566, DOI 10.1016/j.jhydrol.2014.01.064
Liu H, Zhang Y, Zhou Q, Molz F (2007) An interpretation of potential scale dependence of the effective matrix diffusion coefficient. Journal of Contaminant Hydrology 90(1-2):41–57, DOI 10.1016/j.jconhyd.2006.09.006
Liu HH, Bodvarsson GS, Pan L (2000) Determination of particle transfer in random walk particle methods for fractured porous media. Water Resources Research 36(3):707–713, DOI 10.1029/1999WR900323
Maier U, Bürger CM (2013) An accurate method for transient particle tracking. Water Resources Research 49(5):3059–3063
Matheron G, de Marsily G (1980) Is transport in porous media always diffusive? A counterexample. Water Resources Research 16(5):901–917, DOI 10.1029/WR016i005p00901
McCarthy JF (1990) Effective permeability of sandstone-shale reservoirs by a random walk method. Journal of Physics A: Mathematical and General 23(9):L445
McCarthy JF (1991) Analytical models of the effective permeability of sand-shale reservoirs. Geophys J Int 105(2):513–527, DOI 10.1111/j.1365-246X.1991.tb06730.x

McCarthy JF (1993a) Continuous-time random walks on random media. Journal of Physics A: Mathematical and General 26(11):2495–2503, DOI 10.1088/0305-4470/26/11/004
McCarthy JF (1993b) Reservoir characterization : efficient random-walk methods for upscaling and image selection. SPE Asia Pacific Oil and Gas Conference, 8-10 February, Singapore 25334
Metzler R, Klafter J (2000) The random walk's guide to anomalous diffusion: a fractional dynamics approach. Physics Reports 339(1):1–77, DOI 10.1016/S0370-1573(00)00070-3
Metzler R, Glockle WG, Nonnenmacher TF (1994) Fractional model equation for anomalous diffusion. Physica A: Statistical Mechanics and its Applications 211(1):13–24, DOI 10.1016/0378-4371(94)90064-7
Metzler R, Jeon JH, Cherstvy AG, Barkai E (2014) Anomalous diffusion models and their properties: non-stationarity, non-ergodicity, and ageing at the centenary of single particle tracking. Physical Chemistry Chemical Physics 16(44):24,128–24,164, DOI 10.1039/c4cp03465a
Michalak AM, Kitanidis PK (2000) Macroscopic behavior and random-walk particle tracking of kinetically sorbing solutes. Water Resources Research 36(8):2133–2146, DOI 10.1029/2000WR900109
Monaghan JJ (2005) Smoothed particle hydrodynamics. Reports on Progress in Physics 68(8):1703–1759, DOI 10.1088/0034-4885/68/8/R01
Mosé R, Siegel P, Ackerer P, Chavent G (1994) Application of the mixed hybrid finite element approximation in a groundwater model: Luxury or necessity? Water Resources Research 30(11):3001–3012, DOI 10.1029/94WR01786
Narasimhan TN, Pruess K (1988) MINC: An approach for analyzing transport in strongly heterogeneous systems. In: Flow G, Modeling Q (eds) Springer Netherlands, 224, pp 375–391
Néel MC, Rakotonasyl SH, Bauer D, Joelson M, Fleury M (2011) All order moments and other functionals of the increments of some non-markovian processes. Journal of Statistical Mechanics: Theory and Experiment DOI 10.1088/1742-5468/2011/02/P02006
Néel MC, Bauer D, Fleury M (2014) Model to interpret pulsed-field-gradient NMR data including memory and superdispersion effects. Physical Review E 89(6), DOI 10.1103/PhysRevE.89.062121
Noetinger B (2013) An explicit formula for computing the sensitivity of the effective conductivity of heterogeneous composite materials to local inclusion transport properties and geometry. SIAM Multiscale Modeling & Simulation 11(3):907–924, DOI 10.1137/120884961
Noetinger B (2015) A quasi steady state method for solving transient darcy flow in complex 3D fractured networks accounting for matrix to fracture flow. Journal of Computational Physics 283:205–223, DOI 10.1016/j.jcp.2014.11.038
Noetinger B, Estebenet T (2000) Up-scaling of double porosity fractured media using continuous-time random walks methods. Transport in Porous Media 39(3):315–337, DOI 10.1023/A:1006639025910
Noetinger B, Gautier Y (1998) Use of the Fourier-Laplace transform and of diagrammatical methods to interpret pumping tests in heterogeneous reservoirs. Advances in Water Resources 21(7):581–590
Noetinger B, Jarrige N (2012) A quasi steady state method for solving transient Darcy flow in complex 3D fractured networks. Journal of Computational Physics 231(1):23–38, DOI 10.1016/j.jcp.2011.08.015
Noetinger B, Estebenet T, Landereau P (2001a) A direct determination of the transient exchange term of fractured media using a continuous time random walk method. Transport in Porous Media 44(3):539–557, DOI 10.1023/A:1010647108341
Noetinger B, Estebenet T, Quintard M (2001b) Up scaling of fractured media: Equivalence between the large scale averaging theory and the continuous time random walk method. Transport in Porous Media 43(3):581–596, DOI 10.1023/A:1010733724498
Nœtinger B, Artus V, Ricard L (2004) Dynamics of the water-oil front for two-phase, immiscible flow in heterogeneous porous media. 2-Isotropic media. Transport in Porous Media 56(3):305–328, DOI 10.1023/B:TIPM.0000026086.75908.ca
Nunes JP, Bijeljic B, Blunt MJ (2015) Time-of-flight distributions and breakthrough curves in heterogeneous porous media using a pore-scale streamline tracing algorithm. Transport in Porous Media 109(2):317–336, DOI 10.1007/s11242-015-0520-y
O'Brien GS, Bean CJ, McDermott F (2003a) Numerical investigations of passive and reactive flow through generic single fractures with heterogeneous permeability. Earth and Planetary Science Letters 213(3-4):271–284, DOI 10.1016/S0012-821X(03)00342-X

O'Brien GS, Bean CJ, McDermott F (2003b) A numerical study of passive transport through fault zones. Earth and Planetary Science Letters 214(3-4):633–643, DOI 10.1016/S0012-821X(03)00398-4
Odeh AS (1965) Unsteady-state behavior of naturally fractured reservoirs. SPE Journal 5(1):60–66, DOI 10.2118/966-PA
Oliver DS, Cunha LB, Reynolds AC (1997) Markov chain monte carlo methods for conditioning a permeability field to pressure data. Mathematical Geology 29(1):61–91
O'Shaughnessy B, Procaccia I (1985) Diffusion on fractals. Physical Review A 32(5):3073–3083, DOI 10.1103/PhysRevA.32.3073
Ottino JM (1989) The kinematics of mixing: stretching, chaos and transport. Cambridge University Press
Painter S, Cvetkovic V (2005) Upscaling discrete fracture network simulations: An alternative to continuum transport models. Water Resources Research 41(2), DOI 10.1029/2004WR003682
Painter S, Cvetkovic V, Mancillas J, Pensado O (2008) Time domain particle tracking methods for simulating transport with retention and first-order transformation. Water Resources Research 44(1), DOI 10.1029/2007WR005944
Pan L, Bodvarsson GS (2002) Modeling transport in fractured porous media with the random-walk particle method: The transient activity range and the particle transfer probability. Water Resources Research 38(6), DOI 10.1029/2001WR000901
Park Y, de Dreuzy JR, Lee KK, Berkowitz B (2001) Transport and intersection mixing in random fracture networks with power law length distributions. Water Resources Research 37(10):2493–2501, DOI 10.1029/2000WR000131
Park Y, Lee K, Kosakowski G, Berkowitz B (2003) Transport behavior in three-dimensional fracture intersections. Water Resources Research 39(8), DOI 10.1029/2002WR001801
Pichot G, Erhel J, De Dreuzy JR (2010) A mixed hybrid mortar method for solving flow in discrete fracture networks. Applicable Analysis 89(10):1629–1643, DOI 10.1080/00036811.2010.495333
Pollock DW (1988) Semianalytical computation of path lines for finite-difference models. Ground Water 26(6):743–750, DOI 10.1111/j.1745-6584.1988.tb00425.x
Qu ZX, Liu ZF, Wang XH, Zhao P (2014) Finite analytic numerical method for solving two-dimensional quasi-laplace equation. Numerical Methods for Partial Differential Equations 30(6):1755–1769, DOI 10.1002/num.21863
Quintard M, Whitaker S (1993) One- and two-equation models for transient diffusion processes in two-phase systems. Advances in Heat Transfer 23:369–464, DOI 10.1016/S0065-2717(08)70009-1
Redner S (1989) Transport due to random velocity fields. Physica D 38(1-3):287–290, DOI 10.1016/0167-2789(89)90207-8
Risken H (1996) The Fokker-Planck Equation. Springer Heidelberg New York
Rivard C, Delay F (2004) Simulations of solute transport in fractured porous media using 2D percolation networks with uncorrelated hydraulic conductivity fields. Hydrogeology Journal 12(6):613–627, DOI 10.1007/s10040-004-0363-z
Roberts JE, Thomas JM (1991) Mixed and hybrid methods. In: Handbook of Numerical Analysis 2, Finite Element Methods -part 1, Elsevier Science Publishers B.V. (North-Holland), pp 523–639
Robinet JC, Sardini P, Delay F, Hellmuth KH (2007) The effect of rock matrix heterogeneities near fracture walls on the residence time distribution (RTD) of solutes. Transport in Porous Media 72(3):393–408, DOI 10.1007/s11242-007-9159-7
Romary T (2009) Integrating production data under uncertainty by parallel interacting markov chains on a reduced dimensional space. Computational Geosciences 13(1):103–122
Romeu RK, Noetinger B (1995) Calculation of internodal transmissivities in finite difference models of flow in heterogeneous porous media. Water Resources Research 31(4):943–959, DOI 10.1029/94WR02422
Roubinet D, Irving J (2014) Discrete-dual-porosity model for electric current flow in fractured rock. Journal of Geophysical Research-Solid Earth 119(2):767–786, DOI 10.1002/2013JB010668
Roubinet D, Liu HH, de Dreuzy JR (2010) A new particle-tracking approach to simulating transport in heterogeneous fractured porous media. Water Resources Research 46(11), DOI 10.1029/2010WR009371

Roubinet D, de Dreuzy JR, Tartakovsky DM (2013) Particle-tracking simulations of anomalous transport in hierarchically fractured rocks. Computers & Geosciences 50(SI):52–58, DOI 10.1016/j.cageo.2012.07.032

Russian A, Dentz M, Gouze P (2016) Time domain random walks for hydrodynamic transport in heterogeneous media. Water Resources Research, under review

Saffman PG, Taylor G (1958) The penetration of a fluid into a porous medium or hele-shaw cell containing a more viscous liquid. In: Proceedings of the Royal Society of London A: Mathematical, Physical and Engineering Sciences, The Royal Society, vol 245, pp 312–329

Sahimi M (2011) Flow and transport in porous media and fractured rock: from classical methods to modern approaches. John Wiley & Sons

Salamon P, Fernàndez-Garcia D, Gómez-Hernández JJ (2006a) A review and numerical assessment of the random walk particle tracking method. Journal of contaminant hydrology 87(3):277–305

Salamon P, Fernandez-Garcia D, Gomez-Hernandez JJ (2006b) A review and numerical assessment of the random walk particle tracking method. Journal of Contaminant Hydrology 87(3-4):277–305, DOI 10.1016/j.jconhyd.2006.05.005

Salles J, Thovert JF, Delannay R, Prevors L, Auriault JL, Adler P (1993) Taylor dispersion in porous media. determination of the dispersion tensor. Physics of Fluids A: Fluid Dynamics (1989-1993) 5(10):2348–2376

Scher H, Lax M (1973a) Stochastic transport in a disordered solid. I. Theory. Physical Review B 7(10):4491–4502, DOI 10.1103/PhysRevB.7.4491

Scher H, Lax M (1973b) Stochastic transport in a disordered solid. II. Impurity conduction. Physical Review B 7(10):4502–4519, DOI 10.1103/PhysRevB.7.4502

Scher H, Margolin G, Berkowitz B (2002a) Towards a unified framework for anomalous transport in heterogeneous media. Chemical Physics 284(1-2):349–359, DOI 10.1016/S0301-0104(02)00558-X

Scher H, Margolin G, Metzler R, Klafter J, Berkowitz B (2002b) The dynamical foundation of fractal stream chemistry: The origin of extremely long retention times. Geophysical Research Letters 29(5), DOI 10.1029/2001GL014123

Semra K, Ackerer P, Mosé R (1993) Three dimensional groundwater quality modeling in heterogeneous media. In: Water pollution II: Modeling, measuring and prediction, Computational Mechanics Publications, Southampton, UK, pp 3–11

Sen P (2003) Time-dependent diffusion coefficient as a probe of permeability of the pore-wall. Journal of Chemical Physics 119(18):9871–9876, DOI 10.1063/1.1611477

Sen P (2004) Time-dependent diffusion coefficient as a probe of geometry. Concepts in Magnetic Resonance Part A 23A(1):1–21, DOI 10.1002/cmr.a.20017

Sen P, Schwartz L, Mitra P, Halperin B (1994) Surface relaxation and the long-time diffusion coefficient in porous media: Periodic geometries. Physical Review B 49(1):215–225, DOI 10.1103/PhysRevB.49.215

de Simoni M, Carrera J, Sanchez-Vila X, Guadagnini A (2005) A procedure for the solution of multicomponent reactive transport problems. Water Resources Research 41(11), DOI 10.1029/2005WR004056

Srinivasan G, Tartakosky DM, Dentz M, Viswanathan H, Berkowitz B, Robinson BA (2010) Random walk particle tracking simulations of non-fickian transport in heterogeneous media. Journal of Computational Physics 229(11):4304–4314, DOI 10.1016/j.jcp.2010.02.014

Sun NZ (1999) A finite cell method for simulating the mass transport process in porous media. Water Resources Research 35(12):3649–3662, DOI 10.1029/1999WR900187

Sun NZ (2002) Modeling biodegradation processes in porous media by the finite cell method. Water Resources Research 38:3, DOI 10.1029/2000WR000198

de Swaan A (1976) Analytic solutions for determining naturally fractured reservoir properties by well testing. SPE J 16(3):117–22

de Swann A, Ramirez-Villa M (1993) Functions of flow from porous rock blocks. Journal of Petroleum Science and Engineering 9(1):39–48, DOI 10.1016/0920-4105(93)90027-C

Tallakstad KT, Knudsen HA, Ramstad T, Lovoll G, Maloy KJ, Toussaint R, Flekkoy EG (2009) Steady-state two-phase flow in porous media: statistics and transport properties. Physical Review Letters 102(7), DOI 10.1103/PhysRevLett.102.074502

Tang C (1985) Diffusion-limited aggregation and the Saffman-Taylor problem. Physical Review A 31(3):1977–1979, DOI 10.1103/PhysRevA.31.1977

Tang DH, Frind EO, Sudicky EA (1981) Contaminant transport in fractured porous media: Analytical solution for a single fracture. Water Resources Research 17(3):555–564, DOI

10.1029/WR017i003p00555
Tartakovsky AM, Meakin P (2006) Pore scale modeling of immiscible and miscible fluid flows using smoothed particle hydrodynamics. Advances in Water Resources 29(10):1464–1478, DOI 10.1016/j.advwatres.2005.11.014
Taylor GI (1954) Diffusion and mass transport in tubes. Proceedings of the Physical Society Section B 67(420):857–869, DOI 10.1088/0370-1301/67/12/301
Teodorovich E, Spesivtsev P, Nœtinger B (2011) A stochastic approach to the two-phase displacement problem in heterogeneous porous media. Transport in Porous Media 87(1):151–177, DOI 10.1007/s11242-010-9673-x
Tompson AFB, Gelhar LW (1990) Numerical simulation of solute transport in three-dimensional, randomly heterogeneous porous media. Water Resources Research 26(10):2541–2562, DOI 10.1029/WR026i010p02541
Uffink GJM (1985) A random walk method for the simulation of macrodispersion in a stratified aquifer. In: 18th Gen. Assembly Proc. Symp., IAHS Publ. 146, IAHS, Wallingford, UK., Hamburg, Germany
Wang YF, Liu ZF, Wang XH (2014) Finite analytic numerical method for three-dimensional fluid flow in heterogeneous porous media. Journal of Computational Physics 278:169–181, DOI 10.1016/j.jcp.2014.08.026
Warren JE, Root PJ (1963) The behavior of naturally fractured reservoirs. The Society of Petroleum Engineers Journal 3(3):245–255
Wen XH, Gomez-Hernandez JJ (1996) The constant displacement scheme for tracking particles in heterogeneous aquifers. Ground Water 34(1):135–142, DOI 10.1111/j.1745-6584.1996.tb01873.x
Willmann M, Carrera J, Snchez-Vila X (2008) Transport upscaling in heterogeneous aquifers: What physical parameters control memory functions? Water Resources Research 44:12, DOI 10.1029/2007WR006531
Witten TA, Sander LM (1983) Diffusion-limited aggregation. Physical Review B 27(9):5686–5697, DOI 10.1103/PhysRevB.27.5686
Zheng C, Bennett GD (2002) Applied contaminant transport modeling, 2nd edn. 440 pp, Wiley Interscience
Zimmermann S, Koumoutsakos P, Kinzelbach W (2001) Simulation of pollutant transport using a particle method. Journal of Computational Physics 173(1):322–347, DOI 10.1006/jcph.2001.6879